

**Praca wykonana w ramach projektu TEAM
kierowanego przez Prof. Pawła Moskała. Projekt
finansowany przez Fundację na rzecz Nauki Polskiej.**



Uniwersytet Jagielloński w Krakowie

Wydział Fizyki, Astronomii i Informatyki Stosowanej

Zuzanna Bura

Nr albumu: 1124557

**Study of the ortho-positronium mean lifetime
in cancerous and healthy human colon
tissues.**

Praca magisterska
na kierunku biofizyka

Praca wykonana pod kierunkiem

Prof. dr hab. Paweł Moskał

Zakład Doświadczalnej Fizyki Cząstek i jej Zastosowań

Kraków 2020

Acknowledgments

I would like to express my highest gratitude to all people without whom this thesis would not be created.

I would like to thank Prof. Paweł Moskal for time, help, patience, and many valuable remarks that enriched this work. Prof. Stępień and Dr Silarski for the leads and help during conducting the measurements. Mr. Kamil Dulski, Mrs. Ewelina Kubicz for disinterested help in analyzing the results.

Contents

1. Introduction	1
2. Tumors classification	2
3. Basics behind J-PET detector and PALS technique.....	7
3.1. Positron and Positronium	7
3.2. Construction of the J-PET detector	9
3.3. PALS technique	16
3.4. J-PET detector as a device for simultaneous PET and PALS studies.....	19
4. Methods and analysis	20
4.1. Measurements using PALS setup.....	20
4.2. Measurements by means of the J-PET detector	23
5. Results.....	25
5.1. Mean positronium lifetime studies of the fresh samples.....	25
5.1.1. Temperature effect	26
5.1.2. Humidity effect	27
5.1.3. Relation between positronium lifetime and histopathological results	27
5.2. Positronium lifetime of fixed samples	30
5.2.1. Correlation of positronium lifetime and formalin concentration.....	30
5.2.2. Mean positronium lifetime for samples fixed in formalin.....	31

5.3. Relation between positronium lifetime and TNM and G classification.....	33
5.4. Comparison of results from the J-PET detector and PALS setup.....	38
6. Summary and conclusions	40
7. Bibliography.....	42
Appendix A.....	44
Appendix B.....	45

Abstract

Cancer is second cause of death worldwide, currently. The most effective method for cancer prevention is early diagnosis. In this thesis, I describe an innovative method for cancer diagnosis that provides not only information about the localization of tumor in the human body but also about its structure. The main goal of the thesis is to demonstrate the potential of simultaneous PALS (Positron Annihilation Lifetime Spectroscopy) and PET scan (conduct on Jagiellonian Positron Emission Tomograph, developed at the Jagiellonian University). Series of measurements were performed on non-fixed normal and cancerous colon tissue. Studies have shown that within the achieved uncertainties, environmental conditions had no influence on results of mean o-Ps lifetime, unlike formalin, which turned out to have a significant impact. It has been proven that PALS measurements can be made by means of J-PET scanner.

1. Introduction

Cancer is the second leading cause of death globally, affecting the whole human population, however the frequency of a given type of cancer varies depending on age, sex and region. Increasing number of new cases and the most common tumor's types, are associated with the value of the Human Development Index (HDI-is a statistical index that describes life expectancy, education, and per capita income indicators.) [1]. High-resource countries have the highest increase in cancer cases, yet also provides the best health care, including early diagnosis and advanced treatment plans. Cancers of the lung, breast, prostate, and colorectum are the major incident cancers in countries with high or very high HDI. In 2012 worldwide there was 14.1 million new cases of cancer (and 8.2 million deaths). Therefore, the highest incident rate is in Europe (24.4% of new cases and 21.4% of deaths) [1]. It is due to population growth, ageing and modern lifestyle. The prognostics indicate that from 2030 it will be over 20 million new cancer cases per year worldwide [1]. The occurrence of cancer increases with age; differences between sexes are mostly observable over the age of 50. It is because cancer types specific for women (breast and cervical cancer) can occur in an earlier stage of life than cancers specific to men (prostate). The most common types of cancer in Europe are: breast (13.5% cases; 7.5% deaths), prostate (12.1% cases; 5.3% deaths), colorectal (13.9% cases; 12.2% deaths) and lung (11.9% cases; 20.1% deaths) [1].

The majority of modern research focuses on improving human life through the development of novel methods for cancer therapy and diagnosis. With the increasing understanding of cancer biology, not only development of personalized and cancer type targeted treatment is possible, but also a novel method for preventive care and early diagnoses.

One of a novel idea was to combine simultaneous PET (that allows imaging of metabolism rate in the body) and positronium imaging [2]. The mean lifetime of the positronium formed in the sample depends on the size of the free electron spaces that can occur between the molecules and on the concentration of active biomolecules in the cell. Due to these mentioned features, positronium imaging might be used in further research protocols and clinical studies for cancer diagnostic purposes. The purpose of this work is to examine the correlation between ortho-positronium (o-Ps) mean lifetime and the degree of malignancy, size, type of cells and other factors which can be associated with colorectal cancer. Additionally, the goal was to prove that on J-PET scanner enables not only to determine the place of tumor in human body but also to

determine its structures [2]. For this purpose, several measurements of ortho-positronium lifetime in living tissues originating from the large intestine, provided from 2nd Department of General Surgery, Jagiellonian University Medical College in Kraków was conducted. For PALS measurements detectors made from barium fluoride were used, and for PET a new modern tomograph: J-PET, build from plastic scintillators. This work also describes details of measurements and data analysis (chapter 4). Chapter 5 shows the results of PALS measurements on living tissues and tissues fixed in formalin. It describes also the impact of environmental factors such as temperature and humidity on the mean lifetime of o-Ps. The research conducted in the framework of this thesis is concluded in chapter 6.

2.1. Tumors classification.

Cancer

Cancer formation and progression are caused by many superimposed factors, which leads to DNA instability and mutations. Impaired control over cell cycle is caused by mutation in proto-oncogenes, while inhibition in recognizing growth control signals and loss of ability to apoptosis is caused by mutations in suppressor genes. Mutated cells have enhanced proliferation, are undifferentiated and can infiltrate and migrate through blood vessels, causing metastasis [3].

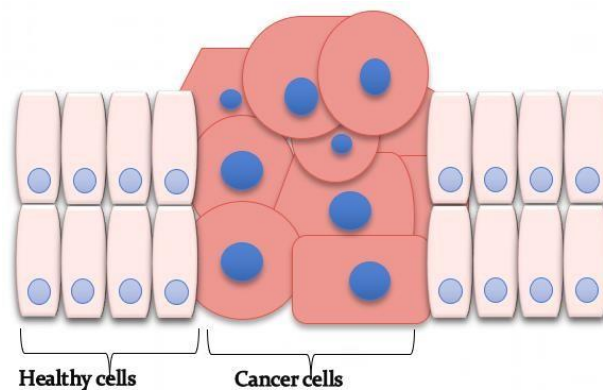


Fig.1. Schematic view of cancer cell arrangement within normal ones. The figure is made by author base on [4]

Cancer cells have not only different structure from normal ones but also have changed and increased metabolism [3][5].

TNM classification

A special classification staging system, called TNM (tumor, nodes, metastasis), is used in medicine to describe differences between cancers. The system is based on anatomical structure of the cancer. It was proposed by Pierre Denoix, and since 1950 the Union for International Cancer Control (UICC) started to use it as a worldwide classification [6]. Nowadays it is the internationally accepted standard for cancer staging [6,7]. The TNM stands for:

Tumor (T) - this category describes the primary tumor size

A scale of 0 to 4 determines the extent of primary tumor growth and its connections with surrounding tissues. The higher the T grade, the more advanced is the cancer [8-9].

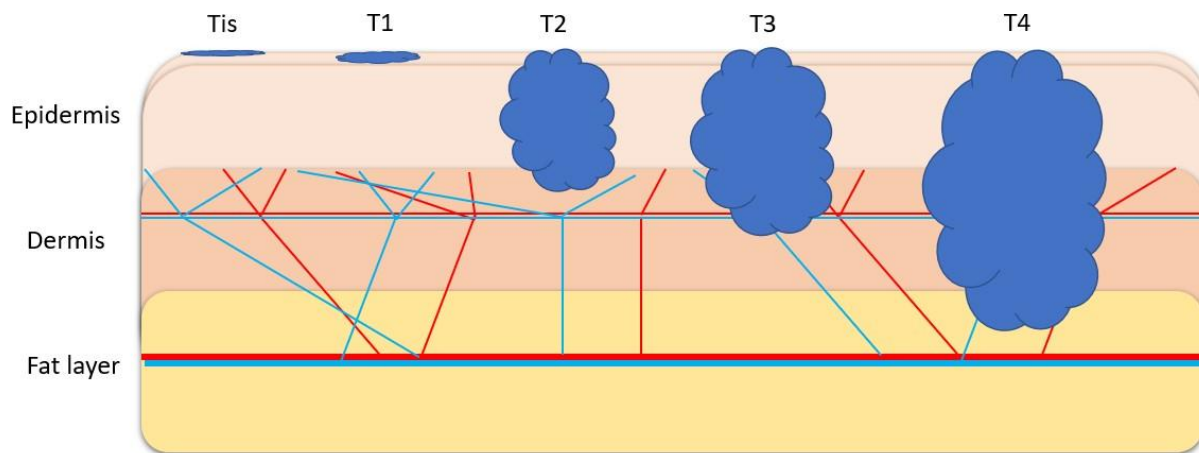


Fig.2. Schematic view of T classification in skin. The figure is made by author base on [10].

The description of the classification goes as follows:

Tx - primary tumor cannot be assessed;

Tis - *cancer in situ* (Cells are contained within one tissue layer).

T0 - no features of the primary tumor.

T1, T2, T3- cancers with adequately larger dimensions.

T4 - a tumor of any size that invades the adjacent organ [10].

Nodes (N)- describes the regional lymph node involvement [6].

The scale from 0 to 3 (for some cancers up to 2 or up to 1). It applies to cancer cells, that invaded lymph vessels from primary tumor and settle. The classification goes as follow:

Nx - cannot be assessed.

N0 - lymph nodes without metastases.

N1, N2, N3, N4 - metastases to lymph nodes increasingly distant from the primary tumor [10].

Metastases (M) - category that describes the presence of distant metastatic the presence or absence of distant metastases throughout the body, with a two-stage scale: 0 for absence and 1 for present metastases [6,10].

In addition to this basic classification, we also distinguish an additional one, that determines the degree of histological malignancy. Combination of these classification allows selecting specific therapy plan and assess patient's prognosis.

Grading (G)- three to four-stage scales of malignancy are usually used depending on the degree of cell differentiation [7].

The classification goes as follow:

GX - the degree of differentiation cannot be assessed.

G1 - highly differentiated cancer (low grade of malignancy).

G2 - moderately differentiated cancer (intermediate grade of malignancy).

G3 - low-differentiated cancer (high grade of malignancy).

G4 - undifferentiated cancer (high grade of cancer malignancy) [10].

Large intestine

Colon is the longest part of the large intestine (typically 150-180 cm long) [11]. In the large intestine individual parts can be distinguished (as shown in Fig. 3):

1. mucosa (includes a columnar epithelium with many mucus-secreting goblet cells, lamina propria (connective tissue) and muscularis mucosa (smooth muscle).
2. submucosa (contains the blood and lymphatic vessels and (Meissner) nerve plexus),
3. muscularis propria (contains the (inner) circular and (outer) longitudinal muscles and myenteric (Auerbach) nerve plexus.),
4. serosa - the outer layer of connective tissue (visceral peritoneum) [11].

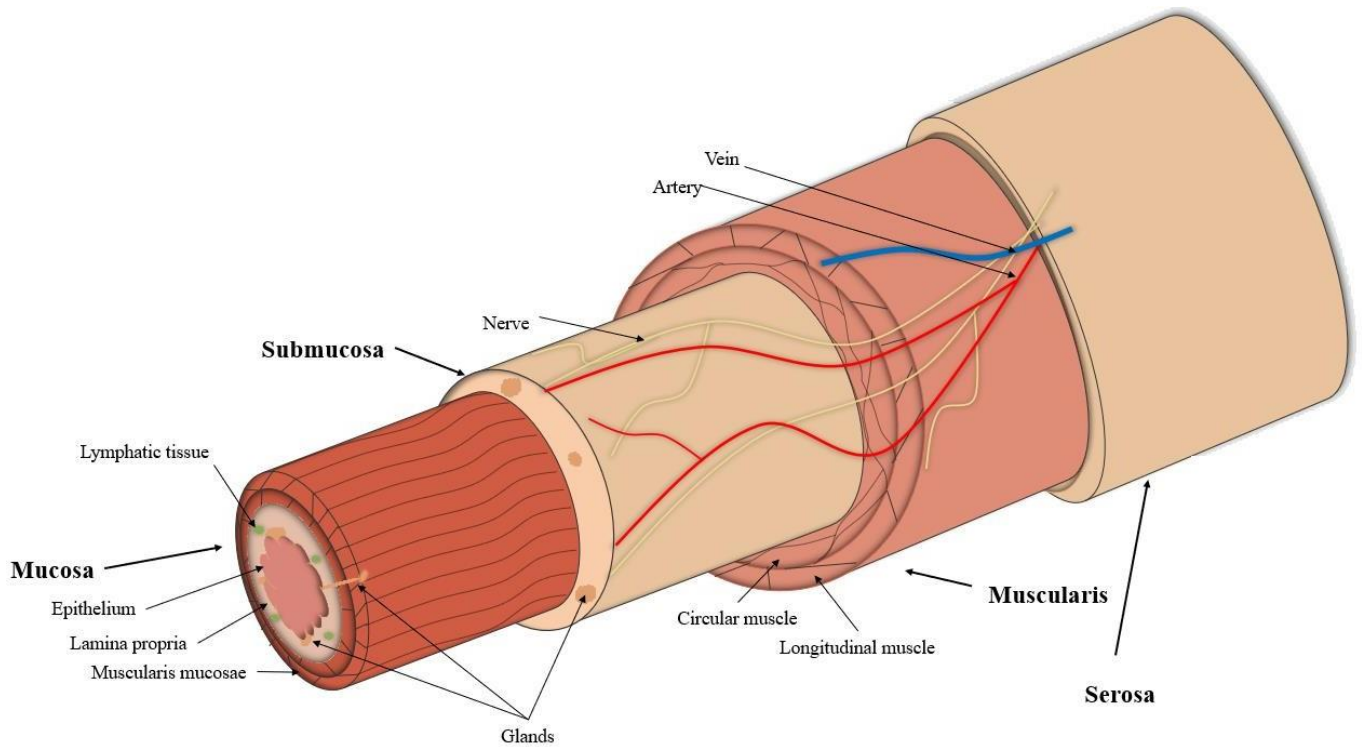


Fig.3. Scheme presenting layers of colon wall. The figure is made by author base on [12].

Colon is the longest part of the large intestine (typically 150-180 cm long) [13].

Colorectal cancer

In 2012 colorectal cancer (CRC) constituted 10% of all cases and thus it was the third most common cancer in men and second in women (with estimated 694 000 deaths in total) [1]. Europe as a highly developing region leads in the number of new cases per year, mostly in central Europe (Slovakia, Hungary and Czech Republic) [1]. The most common environmental factors causing colorectal cancer were: wrong diet, smoking or diabetes, indicating increased incidence is associated with current lifestyles. Especially wrong diet and lack of sports activities, leading to obesity may play a crucial role in mediating carcinogenesis via inflammation [1].

Colorectal cancer is usually identified as adenocarcinoma. Cancer in the right colon is biologically different from that in the left part, in terms of response for treatments and molecular characteristics [1]. The gene responsible for colorectal cancer is the adenomatous polyposis coli (APC). Germ-line mutations in the APC gene result in familial adenomatous polyposis (FAP), one of the principal

hereditary predispositions to colorectal cancer [14]. Adenoma-carcinoma sequence is caused by mutation in four genes. Carcinogenesis pathway of CRC consist of activation of proto-oncogene (KRAS) and inactivation of at least three tumor suppressor genes (mainly APC, TP53, SMAD4) [14]. Macroscopically, tumors have various morphological forms. Ascending colon tumors can occur with an exophytic/fungal growth pattern with the formation of a large polypous mass, often with ulceration. In the descending colon, tumors tend to have a flat, annular growth leading to narrowing of the intestinal lumen [14,15].



Fig.4. Exemplary photography of colorectal cancer specimen.

Colonoscopy is the most commonly used diagnostic method for colorectal cancer, yet around one of two hundred people who undergo this procedure experience a serious complication, like gastrointestinal perforation or bleeding [16].

Early diagnosis, establishing the precise localization and cancer excision before the metastases occur, increases the effectiveness of treatment and increases the chances of recovery. For that reason, it is important to develop a non-invasive and precise diagnostic method of colon cancer.

3. Basics behind J-PET detector and PALS technique

3.1. Positron and Positronium.

The idea of using positron-electron annihilation for medical imaging appeared in the 1950s at the University of Pennsylvania [17]. However, this technique is still strongly developed in modern times [2]. Positron emission tomography is based on the determination of the distribution of radiopharmaceutical in the patient's body. It employs the fact that cancer cells are characterized by increased metabolism. One of the commonly used radiopharmaceuticals in PET scans is ^{18}F - labeled deoxy glucose, which deposits the positron in the patient's body through β^+ decay [18]. Reconstruction of the ^{18}F distribution in the patient's body allows to observe areas with increased metabolism. Positron can interact with free electron via following processes [19][20]:

1. Positron (e^+) after the emission thermalizes in the target and finally is annihilating directly with the electron from the target [21].

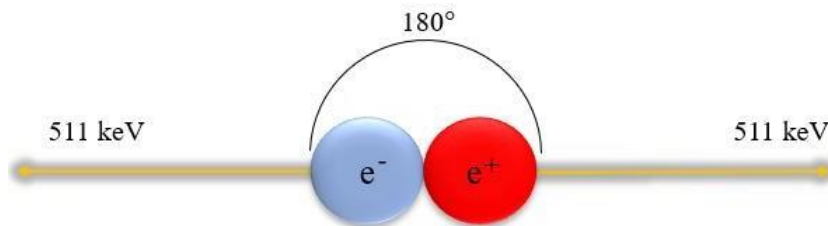


Fig.5. Schematic view of the positronium annihilation resulting in emission of two photons with energy 511 keV

2. Positron after a short thermalization creates a quasi-stable bound state with the electron from the target, that is defined as Positronium (Ps).

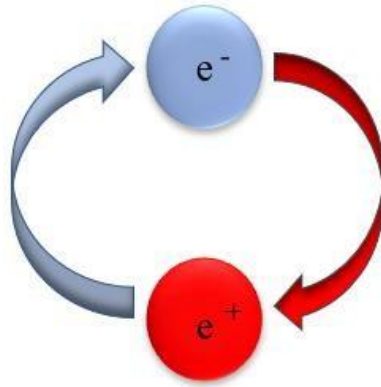


Fig65. Image of positronium molecule. Electron and positron rotating.

Mean lifetime of positronium depends on its total spin number S . Due to the presence of two elementary particles, two types of positronium molecules are distinguished, depending on spin states [20]:

- ◆ Para-positronium (p-Ps) for which the total spin value is $S=0$. P-Ps mean lifetime in vacuum is equal to 125 ps [21].

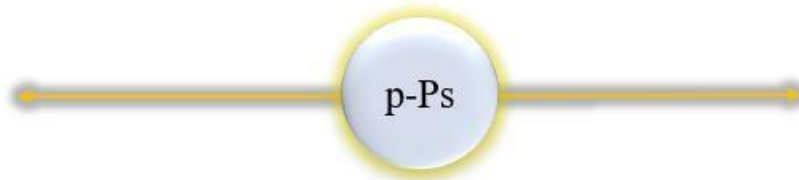


Fig.7. p-Ps deexcitation into two gamma quantum, both with energy equal to 511 keV.

- ◆ Ortho-positronium (o-Ps) (Fig.8) mean lifetime in vacuum is equal to 142 ns, which is three orders of magnitude bigger than mean lifetime of p-Ps [20] [21].

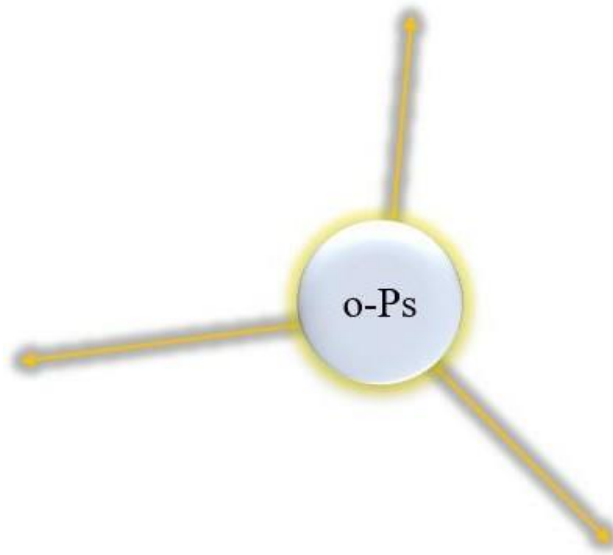


Fig.8. o-Ps deexcitation into three gamma quanta. The value of energy and angles between them, fulfil the law of the conservation of the energy and momentum.

Positronium mean lifetime studies by the PALS technique will be further described in chapter 2.3.

3.2 Construction of the J-PET detector.

Positron Emission Tomography (PET) is one of the methods of cancer diagnosis. Position of the annihilation of the positron and an electron is reconstructed based on the registration of the photons coming from this annihilation [18][19]. Gamma quanta are registered by a set of detectors arranged in a ring. The dimensions of a single detector are on the order of millimeters. Couple of detection rings can be arranged in a cylinder. In usual tomographs number of such rings varies between 6 and 32. Traditional scanners use scintillators made of for example BGO or LSO. Current tomographs usually use crystals with dimensions of several centimeters, cut into smaller elements 0.5 cm x 0.5 cm [22]. A photomultiplier is attached to the crystal.

Principle of the gamma quantum detection is based on the phenomenon of scintillation. The photon hitting the crystal transfers all or part of the energy to the electron, which is knocked out of the atomic shell, then the knocked out electron as a result of ionization and excitation of the atom (or molecules) of the crystal causes a flash of light in it, which by means of a photomultiplier tube is converted into an electric pulse (Fig.9). The impulse created in this way indicates that the particle has passed through the scintillator. The number of photons produced in the scintillator is

proportional to the energy deposited by the gamma quantum. However, the charge of the electric signal generated by the photomultiplier tube is proportional to the number of photons passing through the photomultiplier window [18][23].

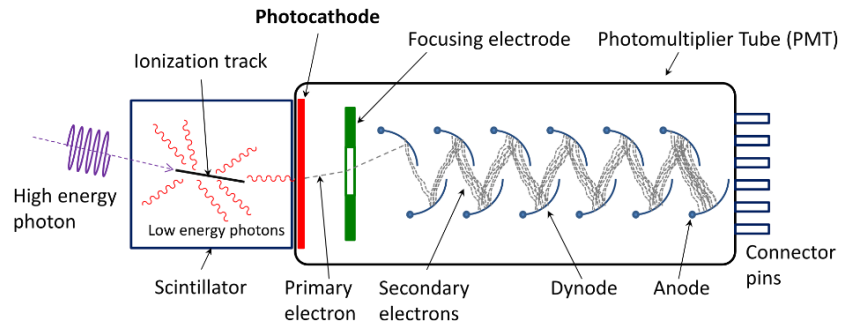


Fig.9. Construction of a scintillation detector consisting of a crystal connected to a photomultiplier. The figure was adapted from [24].

Two phenomena are important for these crystals. The first is (the mentioned before) photoelectric effect, in which the gamma quantum transfers all its energy to the electron. The second is the Compton effect, or so-called Compton scattering, in which gamma quantum transfers some of its energy to the electron and changes its direction (scatter). Compton scattering of annihilation photons in the imaged object reduces the quality of the tomographic image. This defect is suppressed by choosing a scintillator with good energetic resolution, which allows to distinguish annihilation photons with energy of 511 keV from those dispersed in the tested organism as a result of the Compton effect, which have lower energy than them [23].

As a result of annihilation quantum registration, we receive two points at which gamma quanta reacted with detectors. Thanks to this information, we reconstruct the line connecting these points called LOR (Line Of Response) [18][25]. After collecting many such lines, the density distribution of the points where the annihilation occurred is restored (Fig. 10).

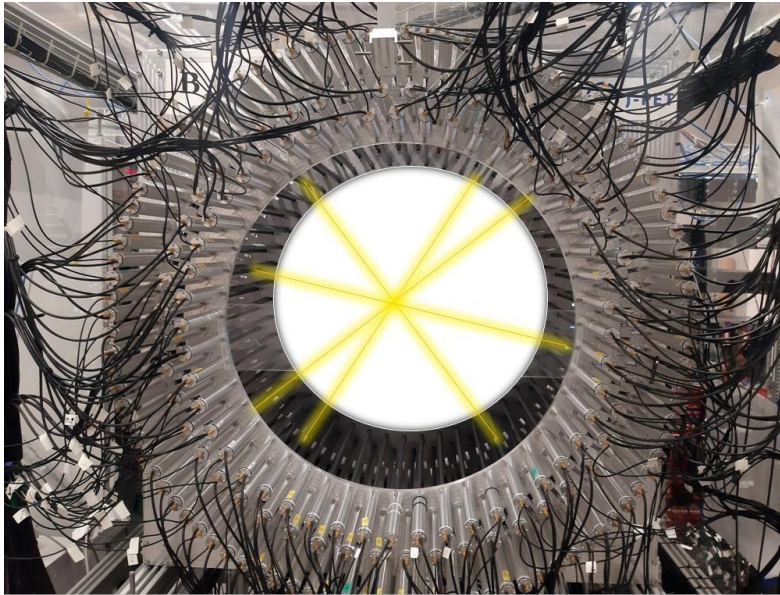


Fig. 10. Photography of a J-PET tomograph with an example of the LOR line inside.

To improve the sharpness of the obtained images, one can employ, the time difference between gamma quanta interaction time (Time of Flight) in detectors.

Research team from the Jagiellonian University headed by prof. Paweł Moskal found an alternative to expensive scintillation crystals, namely a plastic scintillator [19, 25-30] The model of the detection module of the latest prototype scanner is shown in Fig. 11. Jagiellonian PET detector is the first Positron Emission Tomography scanner build from plastic scintillators.

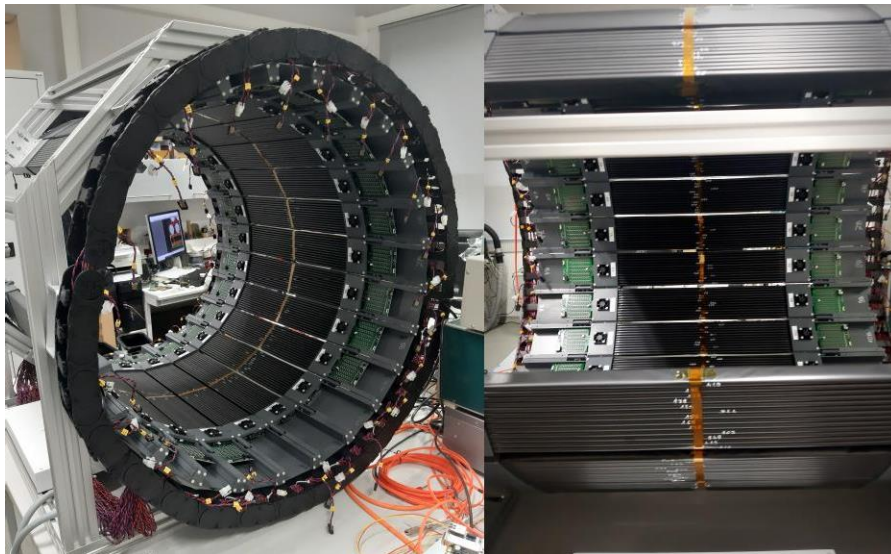


Fig.11. Picture of one of the detection modules of the new J-PET modular scanner. Single detection module consists of 24 detection modules mounted in a metal frame.

In long plastic scintillators, the reconstruction of the image is based on measuring the time of flight. It is useful, following the fact that these materials have much better time properties than crystals [31]. The first prototype of the J-PET real-scale scanner consists of 192 organic scintillation strips that form three coaxial cylindrical layers (Fig. 12), with diameter of 85 centimeters [30]. Thanks to this construction, the acceptance of the apparatus has been increased. Thus, the probability of registering a particle increases, and the final image is obtained from a larger statistic of registered gamma quanta and making it more accurate [30]. Fig. 12 and 13 show the prototype of the J-PET scanner.

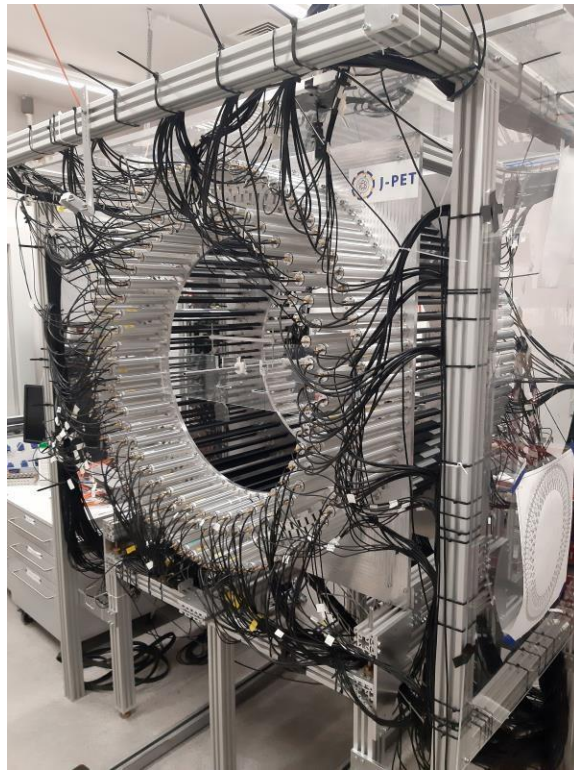


Fig.12. J-PET scanner older version.

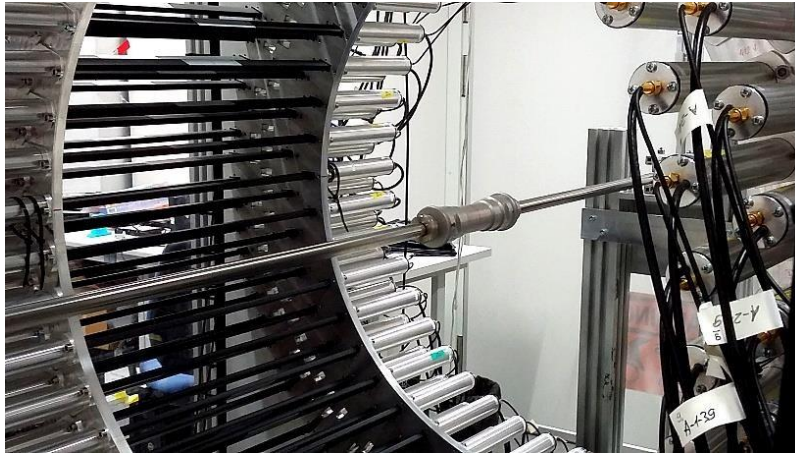


Fig.13. Measurement setup with the aluminum annihilation chamber, placed in the J-PET detector.

In order to compensate for the lower gamma quanta registration efficiency in the organic scintillators more detection layers are used. This together with a large light attenuation length in the plastic scintillators allowed for construction of a tomograph with a large axial field-of-view, cheaper than commercially available scanners. A photomultiplier tube is attached to both ends of each scintillation strip, which converts the light signals produced in the strips into electrical signals. Then, they are processed using special readout electronics and a data acquisition system [32,33].

Consider the event in which gamma quanta are formed in the final state (its source may be different: o-Ps decay, positron-electron annihilation, etc.). The J-PET detector records the interaction of photons with a scintillator. Photon deposits energy in the scintillator, which further propagated in the form of light in each direction (Fig. 14):

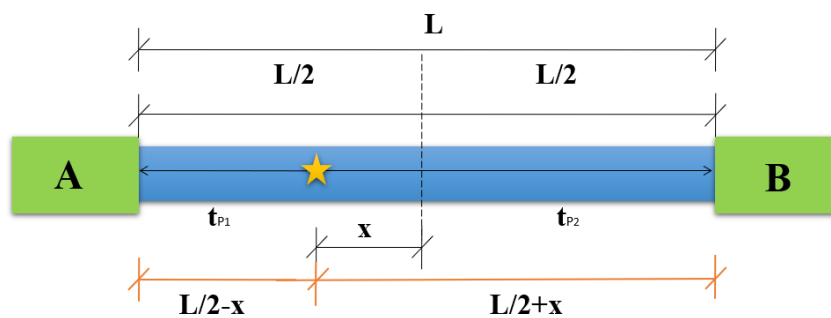


Fig.14. Scheme of the light propagation created in the scintillation process in a L -length detection strip for a gamma quantum that reacted at x . The light reaches the A and B photomultipliers at times t_{P1} and t_{P2} respectively. Figure based on [34].

To determine the place where the gamma quantum deposited energy, related to the center of the scintillator (distant from it of x , as in Fig. 15), it is necessary to determine the difference speed of the light signal v in different materials. For example, in the air v is equal to about 30 cm / ns, when in plastic scintillators it is around 11-12cm / ns [35].

Times recorder at both ends of the J-PET detection module are defined as t_{p1} and t_{p2} according to the Fig. 14. Time can be described as:

$$t = \frac{s}{v} \quad (1)$$

where s is the path taken by the light signal and v is the velocity of the light signal in the scintillator.

The values of t_{p1} and t_{p2} can be written as follows:

$$\begin{aligned} t_{p1} &= \frac{L-x}{v}, \\ t_{p2} &= \frac{L+x}{v}. \end{aligned} \quad (2)$$

Resulting time difference between registration of light signals by two photomultipliers attached to the same scintillator reads:

$$t_{p2} - t_{p1} = \frac{L+x}{v} - \left(\frac{L-x}{v} \right) = \frac{L+x-L+x}{v} = \frac{2x}{v}. \quad (3)$$

It allows to determine the position of the energy deposition as a shift (x) from the center of the scintillator.

$$x = \frac{(t_{p2} - t_{p1})v}{2}. \quad (4)$$

Due to the reconstruction model, accuracy of the determination of the position of the interaction in the scintillator, is closely dependent on the time resolution in the system [35].

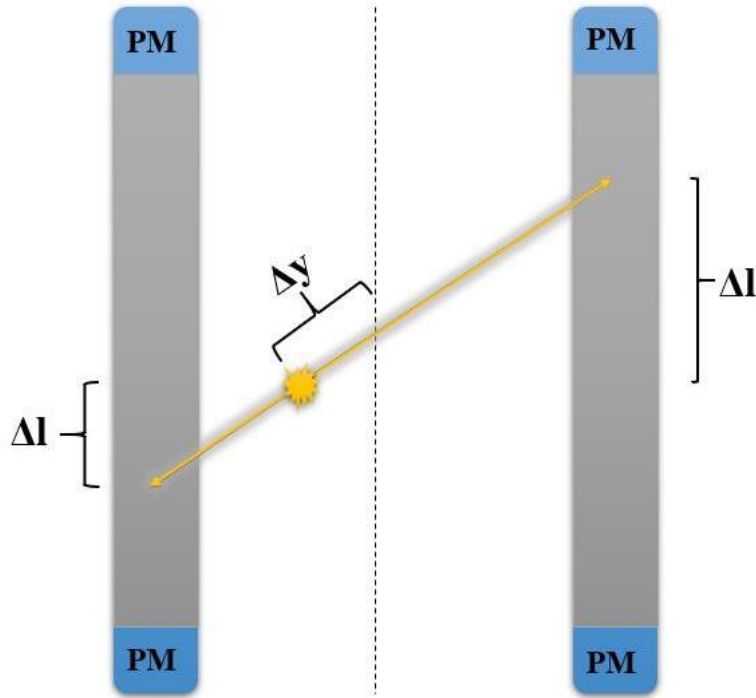


Fig.15. Scheme of the light propagation between two plastic scintillators (LOR line reconstruction). The light reaches scintillators at times t_A and t_B respectively.

The formula analogous to (5) can also be used to determine the place where the o-Ps annihilated and to reconstruct the LOR line (Fig. 15):

$$\Delta y = -\frac{(t_A - t_B)v}{2}, \quad (5)$$

where Δy is the distance of the annihilation site from the center of LOR, and t_A and t_B are the times (averages from the times t_{p1} t_{p2} allocated to the appropriate one detector) [36].

Signals from photomultipliers are sampled using modern electronics on four discrimination thresholds on the rising and falling slope [32-33], which allows to measure widths of the signal on different thresholds closely related to the energy deposited in the scintillator.

The J-PET detector has a trigger-less data acquisition system that records all recorded signals in defined periodic sequences called time windows [35].

Preliminary results indicate that the prototype built at the Jagiellonian University has comparable spatial resolution and twice the time resolution with three times the imaging field (from 17 cm to

50 cm) compared to commercial scanners, thereby minimizing production costs that are the main obstacle to the development of Positron Emission Tomography in Poland [25].

2.3. PALS technique.

Positron Annihilation Lifetime Spectroscopy is a method that describes the dependence of o-Ps mean lifetime on the free electron volumes. It is used to study the structure of materials resulting from molecular packing. As a source of positrons, the ^{22}Na isotope is usually used, which undergoes β^+ decay to ^{22}Ne with emission of positron and neutrino. It is distinguished by the fact that the neon created in this decay is excited, and thus almost immediately (after approx. 3.7 ps) emits a gamma quantum with an energy of about 1274 keV [21,27], which can be used as a signal of the positron creation.. Positron emitted into the sample thermalizes and forms a positronium atom or annihilate directly with one of the electrons from the sample. A diagram of this process is provided in Fig. 7. Positronium, depending on the spin state, can annihilate with emission of two or more gamma quanta. As described in chapter 2.1. However, due to some different process like for example ortho-para conversion or a pick-off, there is a chance that o-Ps annihilates with emission of two gamma quanta and a lower mean lifetime [37]. It was observed that the smaller the free volumes are, the lower is the mean lifetime of o-Ps [38-40]. Changes of the o-Ps mean lifetime reflect changes in the material structure, and therefore they may be connected to the morphology of cells of the living organisms [15,21,26,41-42].

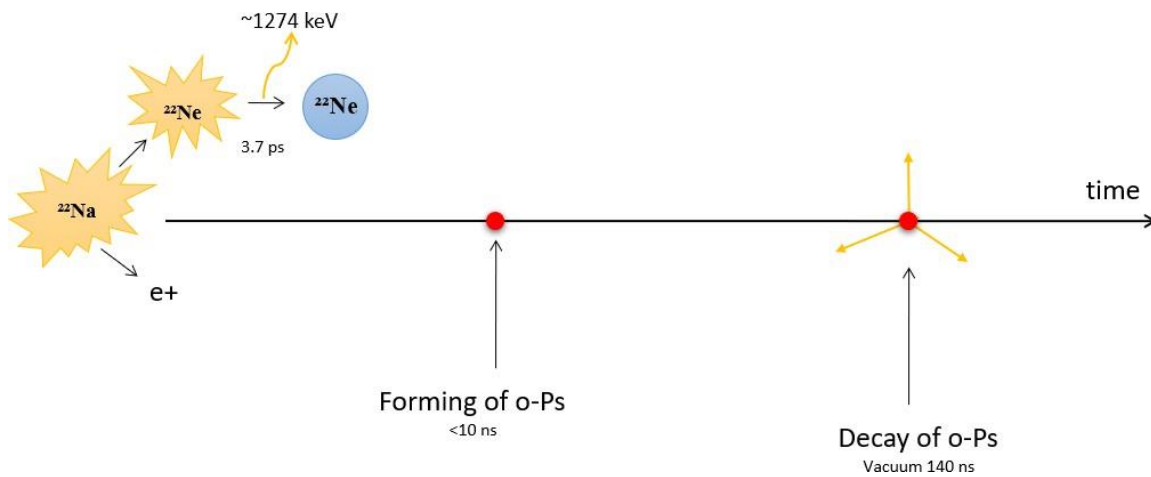


Fig. 16. Schematic representation of the idea of measuring o-Ps lifetime. ^{22}Na decay in β^+ decay and emits positron (which next thermalized) and excited ^{22}Ne which immediately emits energy with the value of 1274 keV. At the same time positron catches electron and form o-Ps, witch then emits three gamma quanta.

To determine the free volumes in the material, the measured mean lifetime of o-Ps can be correlated to the average radius of these volumes using the Tao-Eldrup model [36][40].

The PALS method opens new possibilities for cancer diagnostics. Due to the dependence of the examined lifetime on the material, it will be possible to observe the differences between normal and cancerous tissues, as well as monitor the progress of cancer therapy (diagnostic alternative to biopsy) [26,27,40].

PALS setup usually consists of two crystal detectors characterized by a great time resolution, for example BaF_2 scintillators shown in Fig. 17.



Fig.17. PALS setup consisting of two BaF2 detectors aligned in a collinear manner

The measured samples are inserted between two crystal detectors. Signals from two detectors are read out by the DRS4 digitizer. The scheme of the measurement setup is shown in Fig. 18.

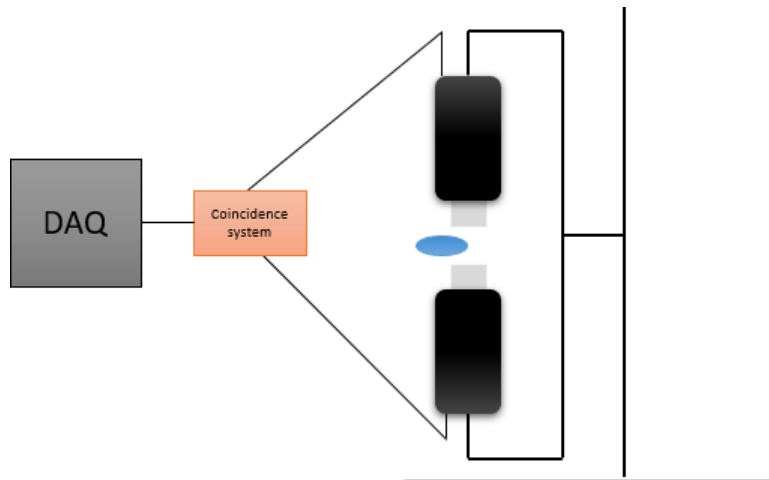


Fig.18. Scheme of PALS setup used for the measurement and its acquisition system. Two crystal detectors are connected to coincidence system and then to the data acquisition system (computer).

3.4. J-PET detector as a device for simultaneous PET and PALS studies

One of the biggest challenges in diagnostic is early recognition of the disease and precise localization of its cause [1]. The PALS technique employs the lifetime and intensity dependence on the structure of analyzed material. Due to this specific feature, PALS might be used in further research protocols and clinical studies for cancer diagnostic purposes. It may also be possible to tell more about the structure of the cancer without a biopsy. By combining the PALS method with Positron Emission Tomography, we can not only precisely localize the cancer even in its early stages but also monitor the effects of therapy. There are many cancers that are difficult to access, which makes it impossible to receive information about them, such as spatial structure or physical properties, such as myxoma located in the ventricles of the heart. Combining the PET and PALS methods will also allow you to receive more information about the structure and location of the tumor, which will open new possibilities in medicine. In addition, o-Ps mean lifetime can change also as a result of electromagnetic interactions of o-Ps with water molecules and other cell-building compounds as proteins or lipids. Thus, mean lifetime of positronium may be different in cancerous and normal tissues due to their different molecular structure [14,21].

But why nobody thinks of that before?

Classical PET has high energy resolution with low time resolution, what complicates it usage in o-Ps lifetime studies the time resolution for classical PET is 390 ps [43], that is slightly less than the o-Ps mean lifetime for water (1.8 ns) [21]. The J-PET detector in principle offers superior time properties (resolution better than 100ps [44]) that allows to study change in o-Ps lifetime in different structures. In Fig.19 the combination of PET and PALS is shown.

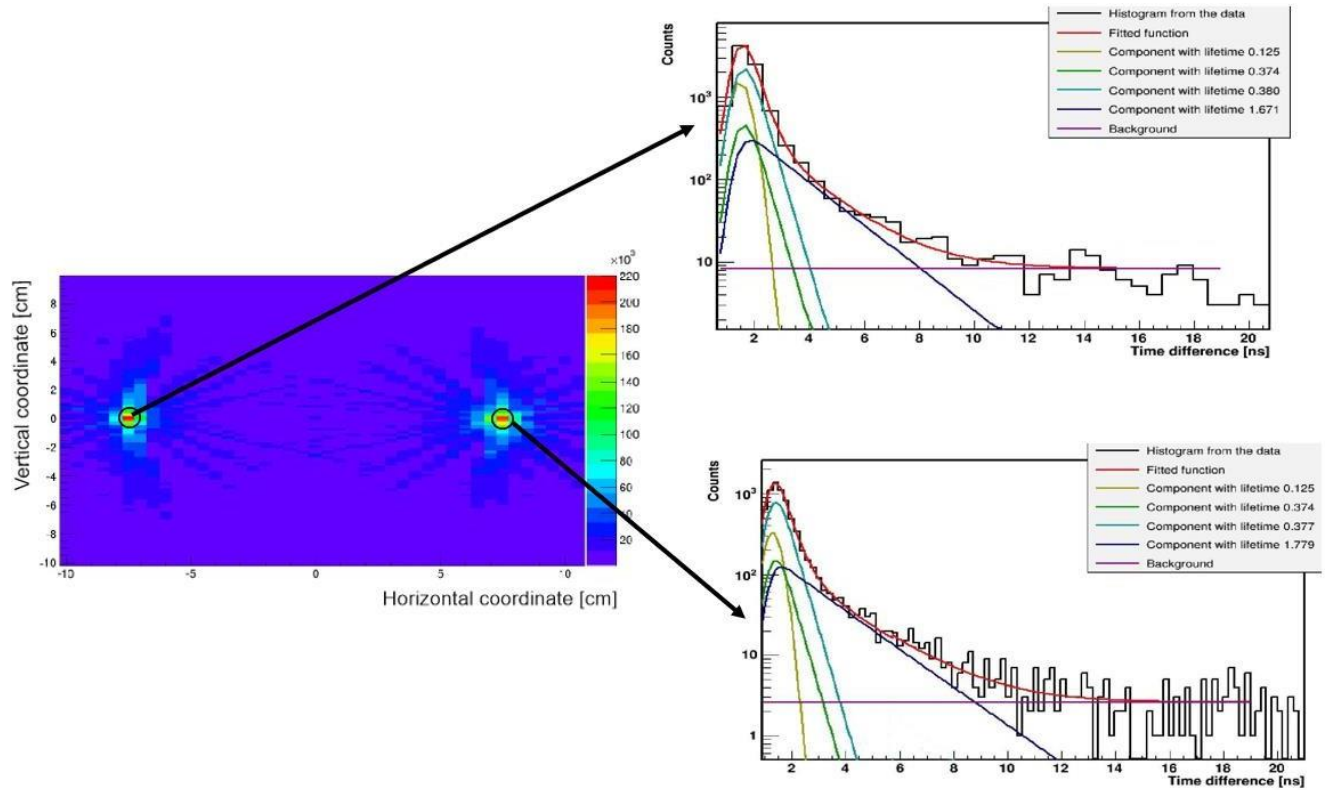


Fig. 19. (left) Density distribution of points in the XY plane received from positron-electron annihilation during measurement with J-PET. (right) Resulting positron lifetime distributions for (top) cancer sample and (bottom) normal sample.

4. Methods and analysis

4.1. Measurements using PALS setup

The goal of these measurements is to determine the lifetime of o-Ps in human tissue to establish the correlation between orth-positronium (o-Ps) mean lifetime and the structure of the large intestine cancer. It will allow to recognize the degree of malignancy, size, type of cells and other factors already during body imaging and without violating patients' purtenance. The sooner the features of cancer will be known, the sooner appropriate treatment can be applied. Research presented in this thesis are based on the agreement of the Bioethical Committee of the Jagiellonian University no. 1072.6120.13.2019. Studied samples originating from the large intestine (normal and cancer tissue) and were delivered from 2nd Department of General Surgery, Jagiellonian University Medical College in Kraków. Samples were transported in a thermally isolated bag with

special containers with solution of PBS without Ca^{2+} , Mg^{2+} [45]. For the studies all patients with colorectal cancer were accepted, the only excluding criteria were: size of tumor (if smaller than 1 cm^3) and positive tests for HIV, hepatitis B and C.

For the measurements, obtained normal and cancer samples were cut into two parts (Fig. 20) and placed in aluminum chambers with ^{22}Na radioactive source (1Mq) sealed in $0.6 \mu\text{m}$ thick Kapton foil source between them (Fig. 20).



Fig.20. Photographs illustrating sample preparation and mounting in chamber with radioactive source. Firstly the sample is cutted, then placed in holder with the source and at the end siled with paralim [45].

Chamber with sample and source was then inserted between two BaF_2 scintillators as shown in Fig. 21.

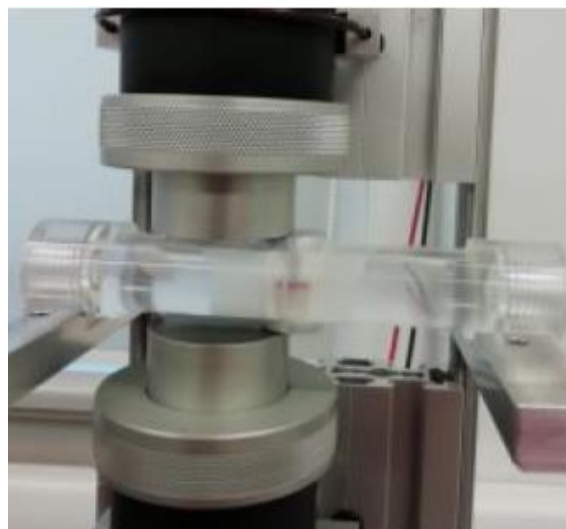


Fig.21. Photograph presenting the PALS detectors and assembled chamber with sample between them.

Firstly, cancer sample is measured and then normal one. Every measurement last one hour, after which tissues were placed in 4% formalin solution.

Mean positronium lifetime is estimated from lifetime distribution. The analysis was performed by the PALS Avalanche software [46,47]. In Fig.22 exemplary positronium lifetime spectrum with fitted model and components of given type of positronium annihilation, is presented.

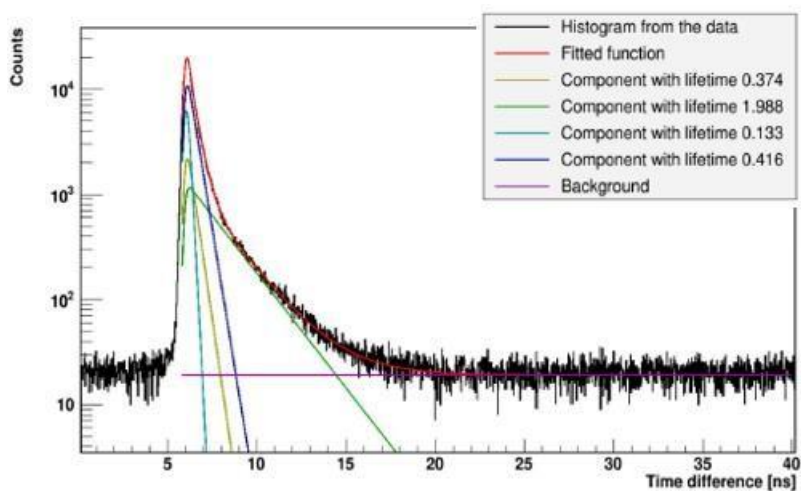


Fig.22. Exemplary PAL spectrum for a cancer sample. Red curve indicates model fitted to the positron lifetime distribution. It consists of a contribution originated from the detection setup itself (due to its time resolution) constant background (purple) and a set of exponential functions originating from positron annihilation: o-Ps decay (green), free positron annihilation (blue), annihilation in the source itself (olive green) and p-Ps decay (light blue).

4.2. Measurements by means of the J-PET detector.

This part of the experiment was designed to verify the application of positronium lifetime in cancer diagnostics during simultaneously PALS/J-PET measurement. In this case pairs of normal and cancer tissue of the same patient, previously fixed in formalin, were measured at the same time using special holder shown in Fig. 23. In these measurements, two ^{22}Na sources were used, one with activity 0.77 MBq (cancer) and the other 0.61MBq (normal).

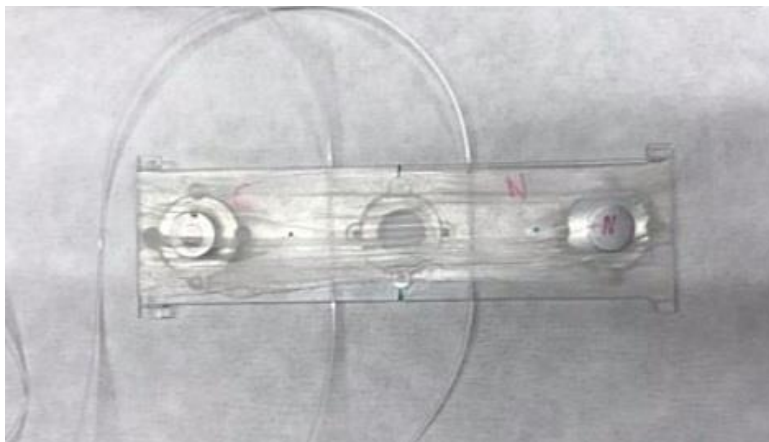


Fig.23. Holder with chambers.

Study group consisted of 27 patients, what gives in total 54 samples.

Samples, after being removed from the formal solution were thoroughly dried on paper towel. Two part of each normal and cancer tissues were placed in the chambers. Firstly, the lower part was placed in holder with the source and at the end the upper part. Cancer on the left side and normal on the right (Fig. 24)

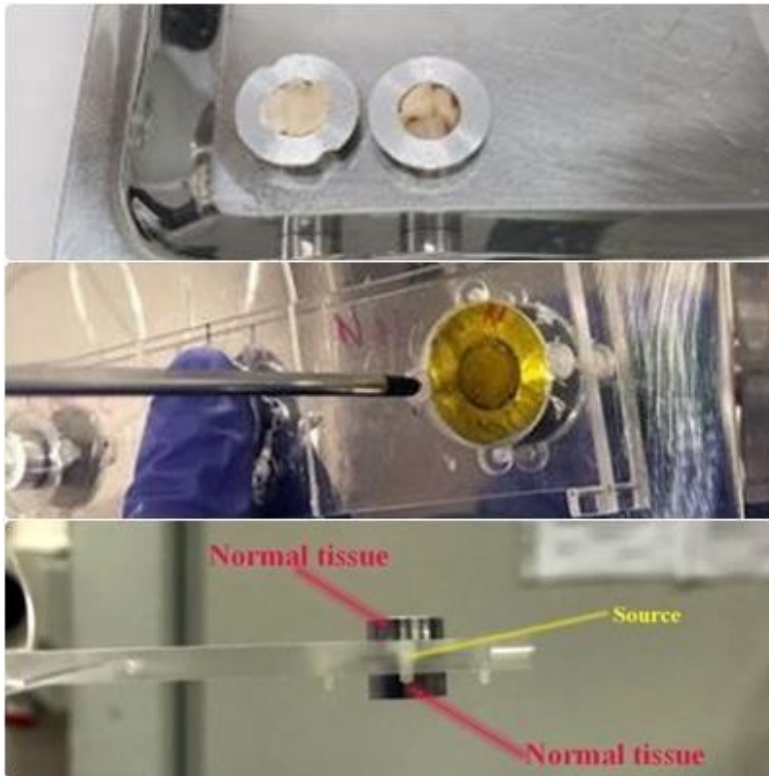


Fig.24. Photographs presenting method of chamber assembly with samples and radioactive sources.

Samples were inserted in the J-PET detector in the position $(0, 7.5, 0)$ for cancer and $(0, -7.5, 0)$ for normal sample, therefore distance between the sources were 14.8 cm.

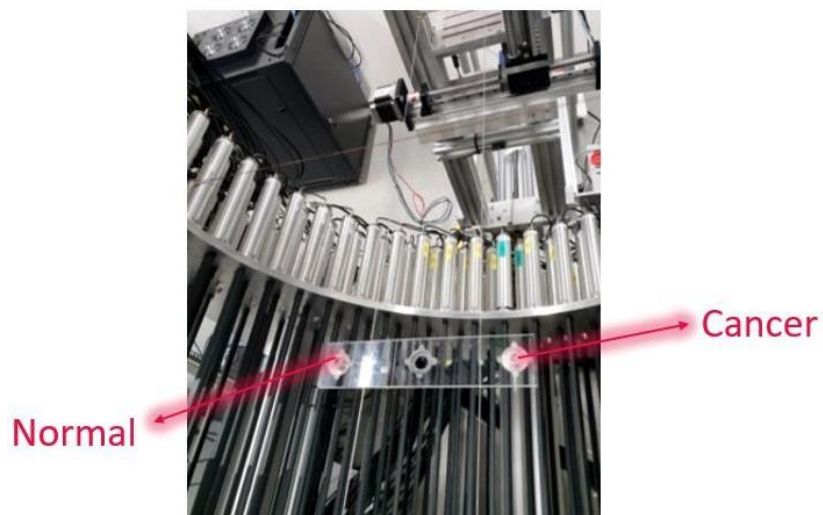


Fig.25. Photography of the sample with source in holder in J-PET.

Conducted measurements lasted from 8 hours to 64 hours depending on the sample.

5. Results

5.1. Mean positronium lifetime studies of the fresh samples.

Studies on non-fixed normal and cancer large intestine tissue were conducted on specimens from forty patients. The o-Ps lifetime for each of them is presented in Figure 26.

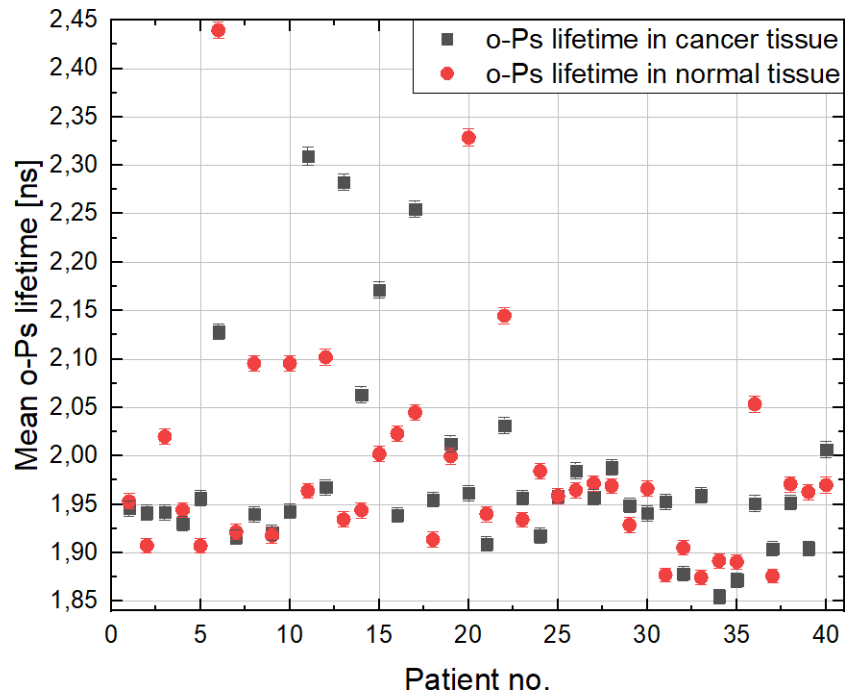


Fig.26. Mean o-Ps lifetime for cancer and normal large intestine tissue

In 18 cases differences in mean o-Ps lifetime between patients is observed (o-Ps lifetime in cancer is higher than in normal cells), yet obtained results are not consistent from patient to patient. These discrepancies may be caused by some external environmental factors or the diversity in the study. The variety of the results between each patient may also come from different lifestyle factors like obesity (10 patients), smoking (6 patients), diabetes (8 patients) or cardio-vascular diseases (22 patients). Most of the results fluctuate around 1,95 ns.

To determine the influence of temperature and humidity on positronium lifetime, series of measurement in different conditions were performed. Influence on detector resolution of changing temperature and humidity in the laboratory, was estimated.

5.1.1. Temperature effect

The temperature was set on the air conditioner in the laboratory and then checked on the sensor located close to the detector. To obtain temperature spread, measurements were conducted at different times during a day. In Fig. 27 the dependence of detector resolution on temperature is presented.

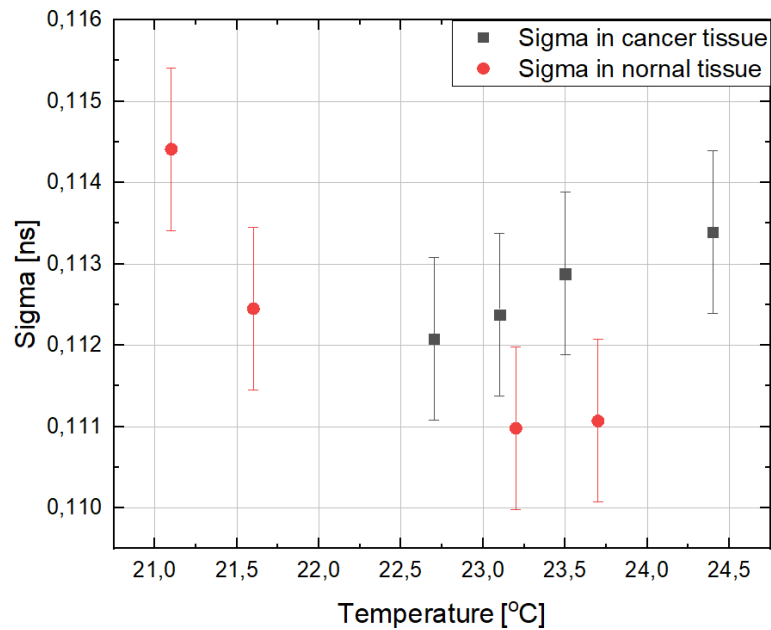


Fig.27. Dependence of temperature on detector resolution (sigma).

All of the discrepancies in the results are within the limits of errors bars.

5.1.2. Humidity effect.

Humidity was also checked on the same sensor as the temperature and the measurements were conducted at different times of the day. In Fig. 28 results of dependence of detector resolution on humidity.

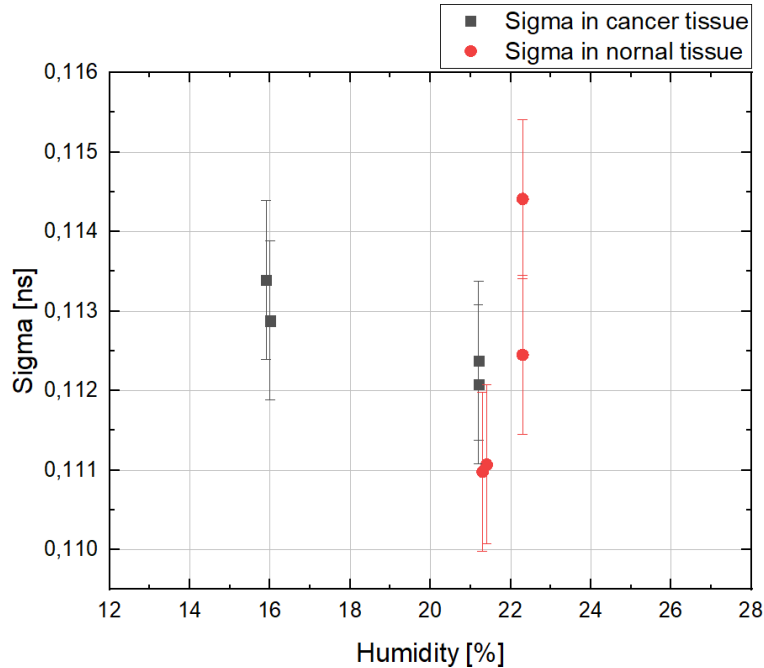


Fig.28. Humidity dependence on detector resolution (sigma).

In both cases no significant influence on detector resolution by changing environmental conditions was observed.

5.1.3. Relation between positronium lifetime and histopathological results

Histopathology examination of normal and cancer specimens obtained for PALS experiment was performed for 27 patients. Due to obtained results samples were divided into three groups. The division has been made due to discrepancies between expectations (based on observations of doctors) and what was observed in the histopathological examination: (1) sample consisted mostly of expected tissue type (mostly normal muscularis cells or mostly cancerous cells), (2) given sample contained other types of cells, (3) most of the sample constituted of improper cell types. The example of each group is presented in Fig. 29 and Fig. 30.

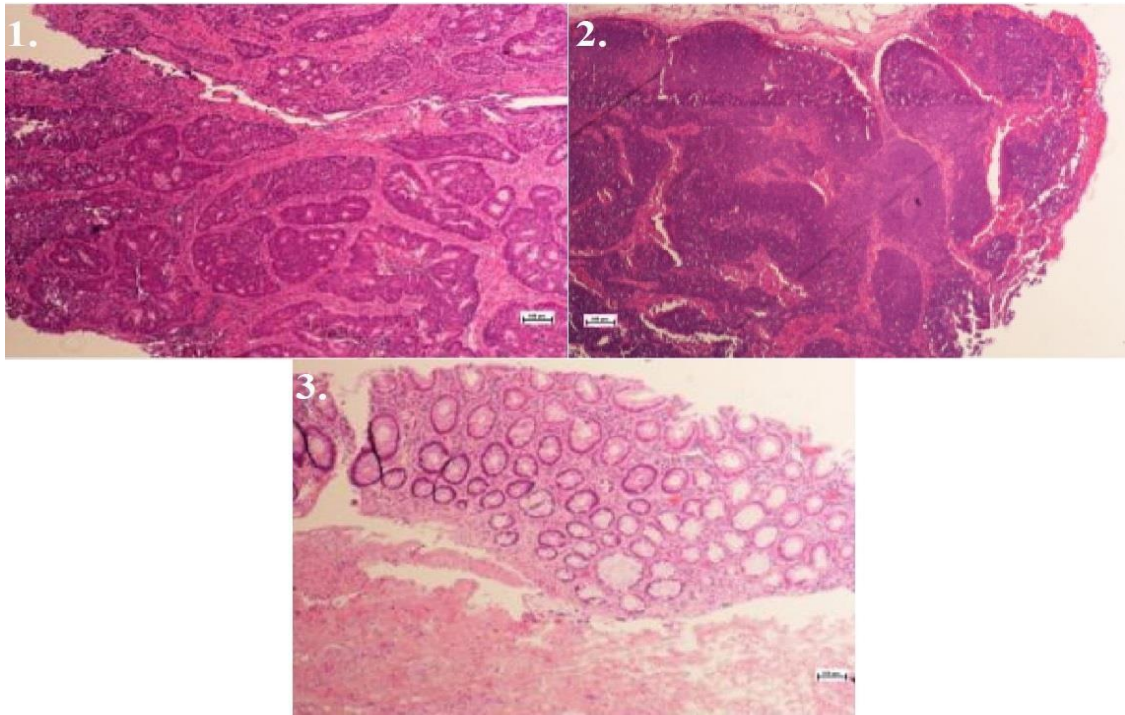


Fig.29. Microscopical cancer tissue image of representation of each histopathological group. As follows 1. For the first group, 2. for the second and 3. for the last one. Scale bar is equal to 100 μm . [48]

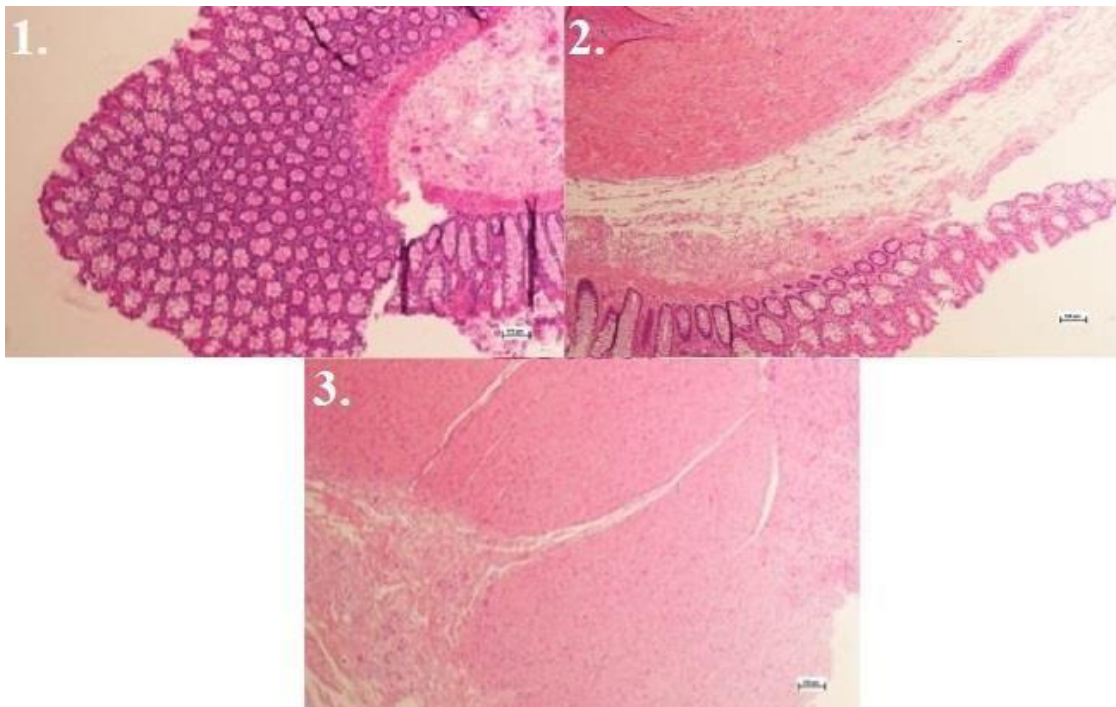


Fig.30. Microscopical normal tissue image of representation of each histopathological group. As follows 1. For the first group, 2. for the second and 3. for the last one. Scale bar is equal to 10 μm . [48]

The studied cancer was adenocarcinoma. It is defined as neoplasia of epithelial tissue. However, healthy tissues compared were mainly from lamina muscularis, only one sample (from patient number 12) differs from submucosa. The mean o-Ps lifetime for each patient from 1 group are shown in Fig. 31.

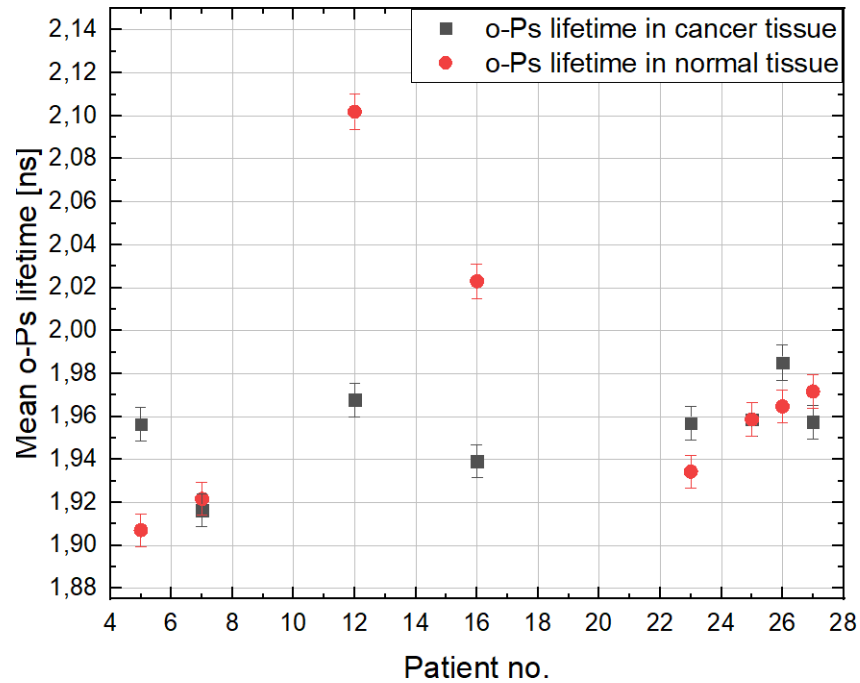


Fig.31. Mean o-Ps lifetime in normal and cancer tissues for specimens from 1 group.

In Fig. 32 mean o-Ps lifetime for specimens from first and second group of histopathology results.

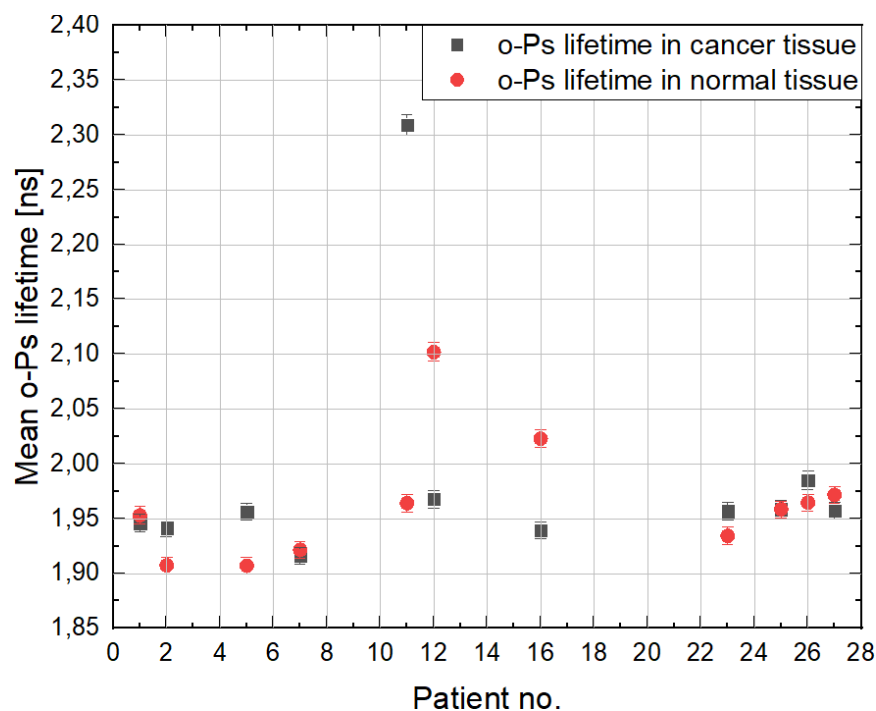


Fig.32. Mean o-Ps lifetime of normal and cancer tissues for specimens from 1 and 2 group.

Based on graphs presented above it is visible that most of the determined o-Ps mean lifetimes are in the range between 1.90ns and 1.97ns, while only in three cases the obtained values are much higher. Moreover, no clear differences between o-Ps mean lifetime of healthy and cancerous tissues is observed.

5.2. Positronium lifetime of fixed samples.

5.2.1. Correlation of positronium lifetime and formalin concentration.

Specimens after PALS experiment were fixed, after measurements are fixed in 4% formalin (the 100% solution of formalin is 36-40% solution of formaldehyde). To prepare this solution, 38-40% Formaldehyde is mixed with PBS in a ratio of 1:10.

Five solutions of different formalin concentrations were prepared: 0% (PBS), 2.5%, 10%, 40% and 100%. Source for these measurements was wrapped in a parafilm to avoid leaking. Contribution of parafilm on positronium lifetime was subtracted from the final results. After measurements, the formalin solutions were put back to the fridge and after 150 days the second trial of the same measurements were performed. Results are shown in Fig 33.

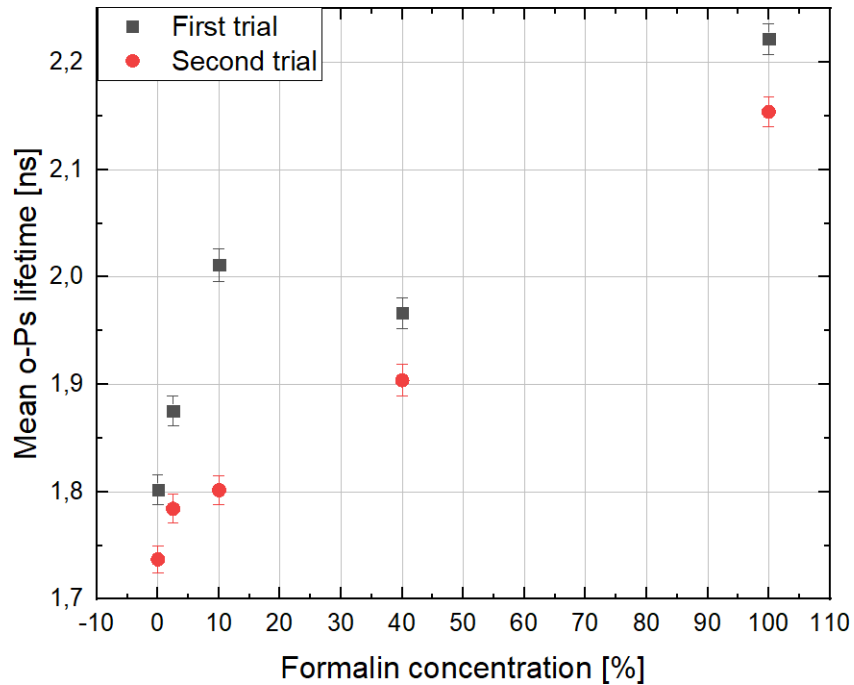


Fig.33. o-Ps lifetime dependency on formalin concentration

The mean o-Ps lifetime increases with the concentration of formalin. Around 40% saturation occurs, and then again, a significant increase of mean o-Ps lifetime value. For 4% solution (which is the solution, used for fixation of measured in this thesis samples) it is equal to around 1.8 ns. Formalin "freshness" is also important, but the solution used to fix the samples is prepared anew every month.

5.2.2. Mean positronium lifetime for samples fixed in formalin.

After fixation samples were measured again on PALS detectors, to compare the difference between fixed and non-fixed tissues. The results for all tissues are shown in Figure 34, while Figures 35 and 36 show the results for group 1 and 2 classified based on histopathological assessment.

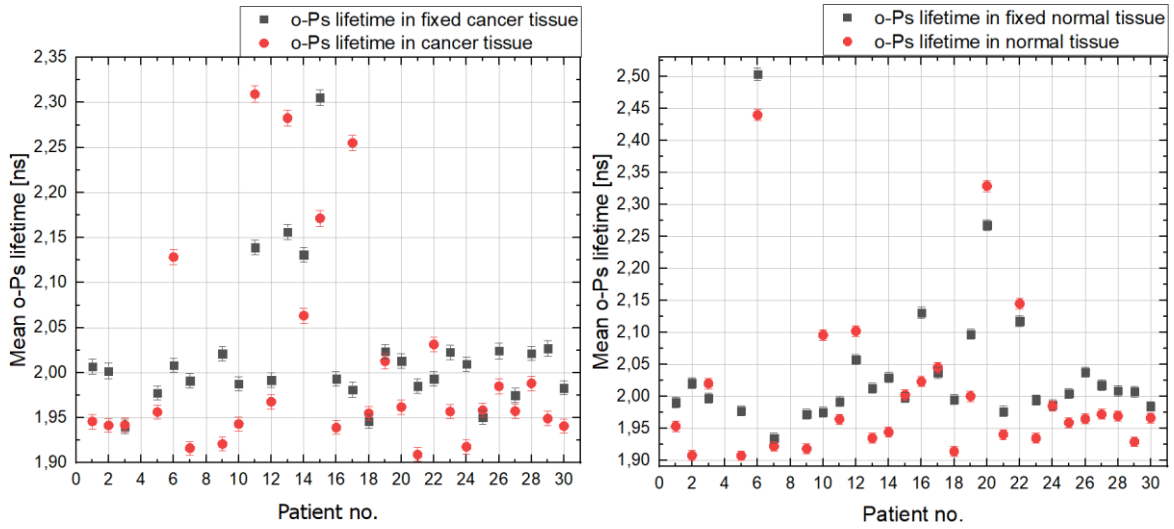


Fig.34. On the left side the results for cancer are presented (23 (of 28) cases when fixed samples had similar or higher lifetime than no fixed) and on the right side for normal tissues (23 (of 28) cases when fixed samples had similar or higher lifetime than no fixed)

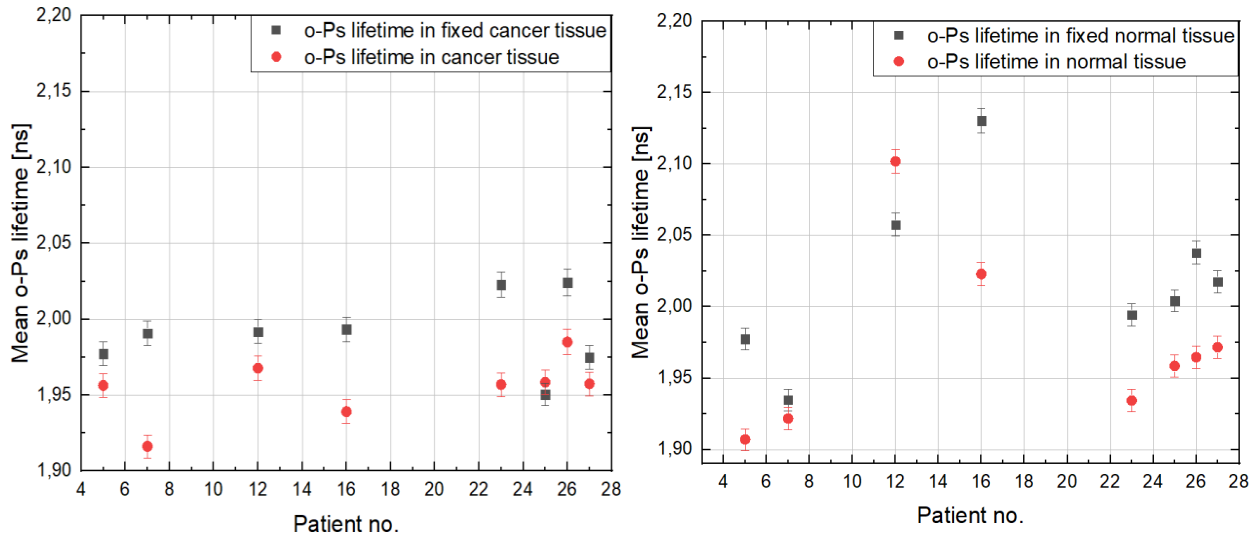


Fig.35. Results for samples 1 group of histopathology results. On the left side the results for cancer are presented (8 (of 8) cases when fixed samples had similar or higher lifetime than no fixed) and on the right side for normal tissues (7 (of 8) cases when fixed samples had similar or higher lifetime than no fixed).

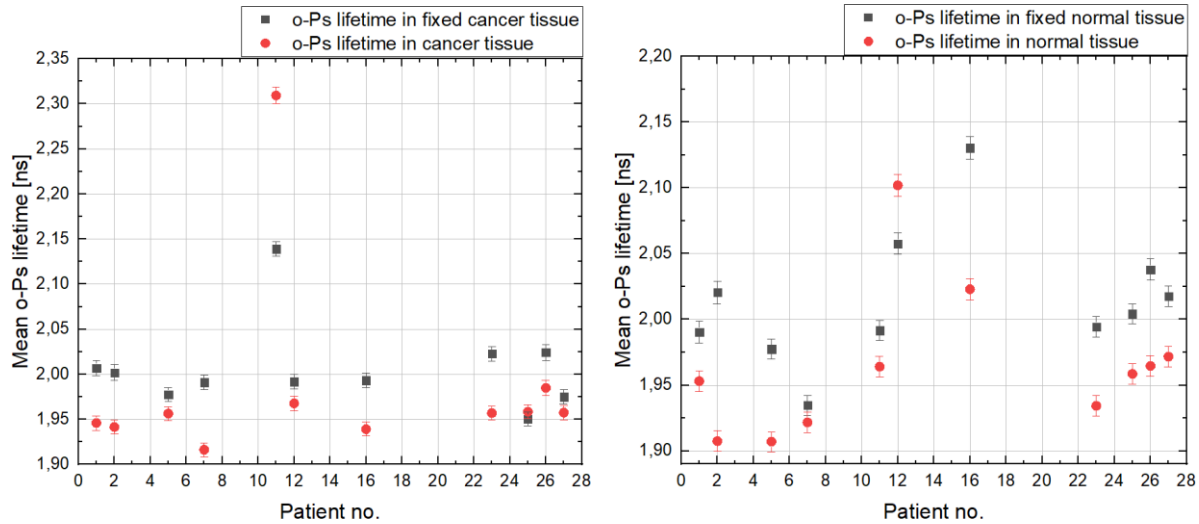


Fig.36. Results for samples for the second group of histopathology results. On the left side the results for cancer are presented (10 (of 11) cases when fixed samples had similar or higher lifetime than no fixed) and on the right side for normal tissues (10 (of 11) cases when fixed samples had similar or higher lifetime than no fixed).

Samples fixed in formalin shows growth of mean o-Ps lifetime value. 82% of cancer and normal tissues fixed in 4% formalin solution had higher lifetime than fresh ones (measured the same way on the same detector). After including histopathological results, the percentage increased.

5.3. Relation between positronium lifetime and TNM and G classification

TNM staging system as mentioned in chapter 2 is a special classification used in medicine to describe differences between cancers. Primary tumor size (T), regional lymph node involvement (N) and the presence of distant metastatic spread (M).

Results of mean o-Ps lifetime including T classification are presented in Fig. 37 and 38.

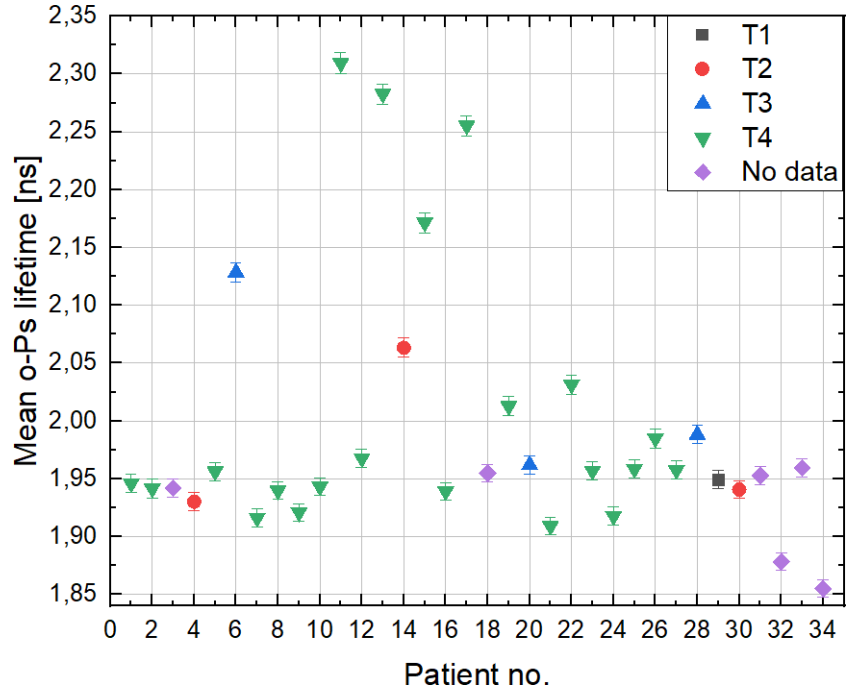


Fig.37. o-Ps dependency of different T characteristic for all patients

After including histopathology results:

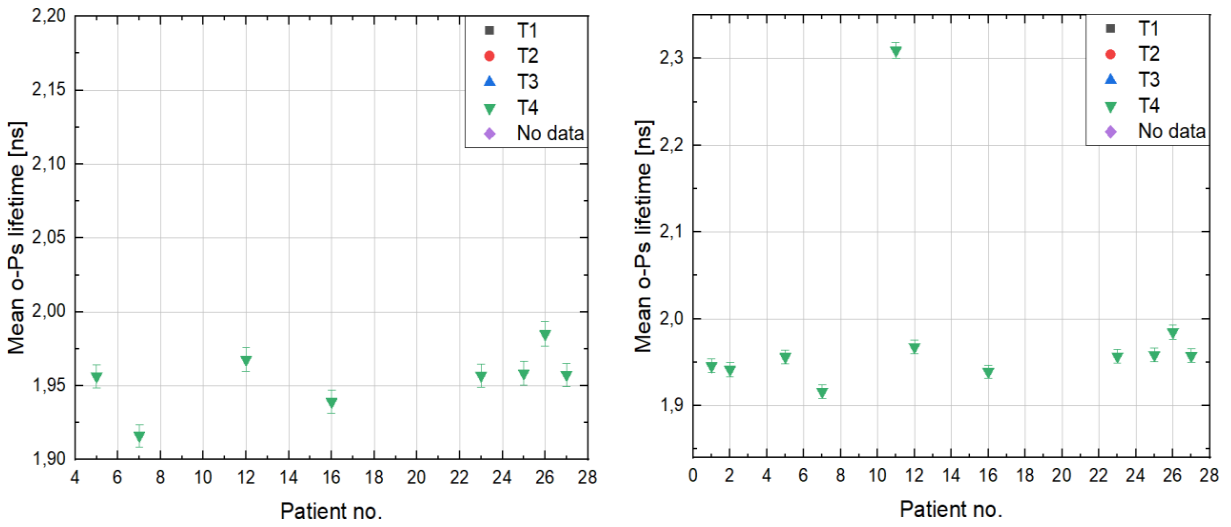


Fig.38. o-Ps dependency of different T characteristic, after including histopathologic results. On the left graph for good results and on the left the average one's were added.

For N classification results are presented in graphs 39 and 40.

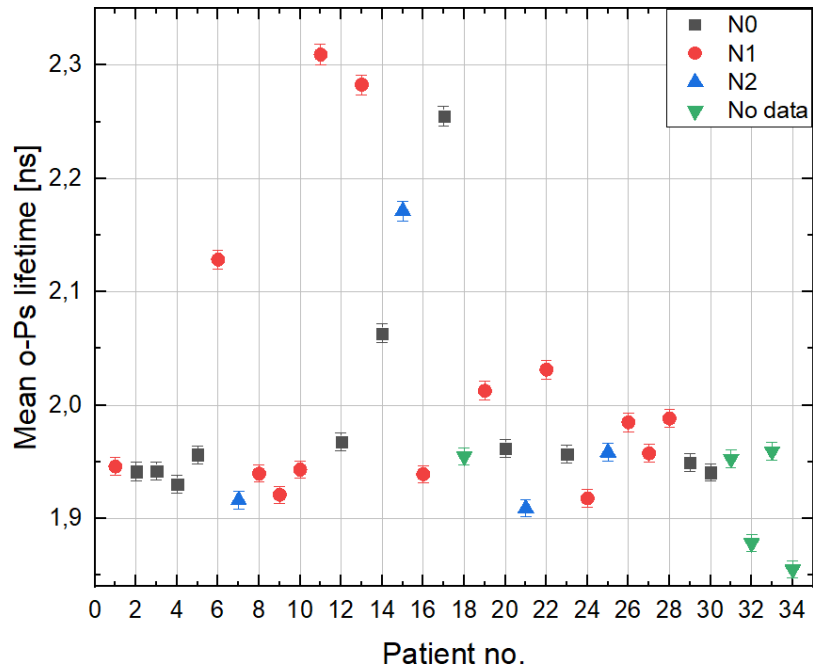


Fig.39. o-Ps dependency of different N characteristic for all patients

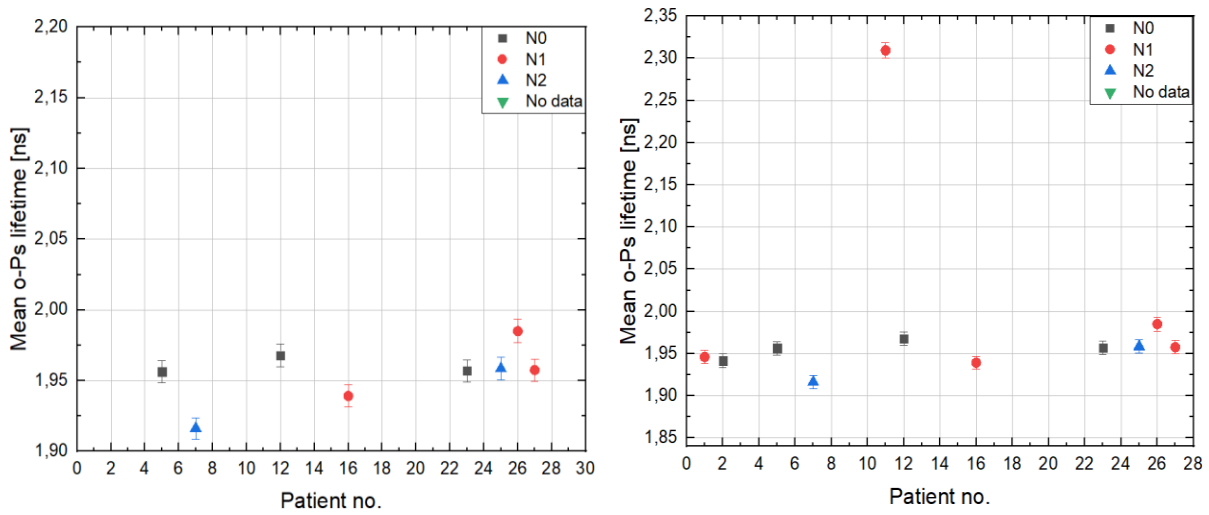


Fig.40. o-Ps dependency of different N characteristic, after including histopathologic results. On the left graph for good results and on the left the average one's were added.

In Fig. 40 three patients (23, 25, 27) with different number on N scale have exactly the same o-Ps lifetime.

For M classification results are presented in graphs 41 and 42

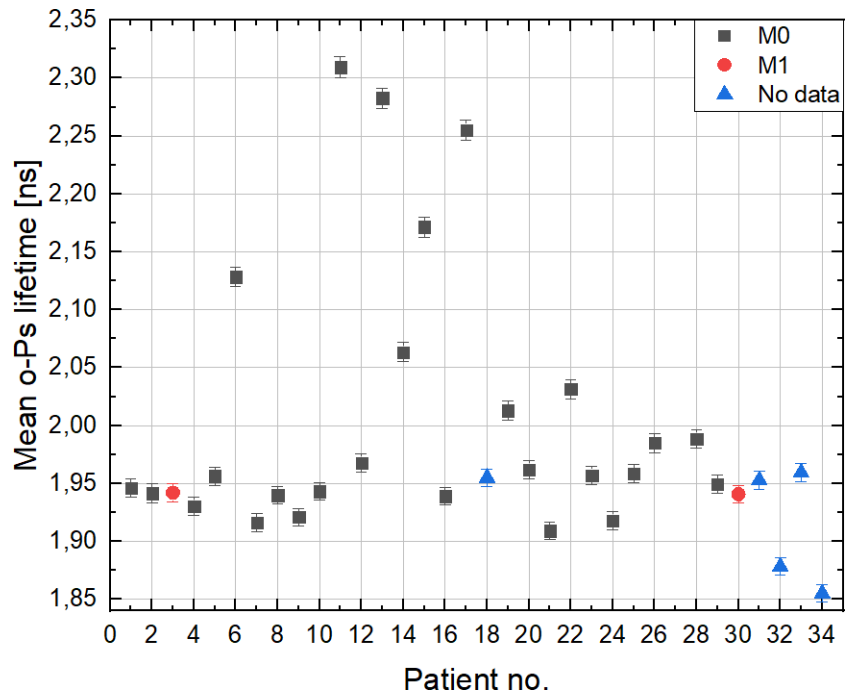


Fig.41. o-Ps dependency of different M characteristic for all patients

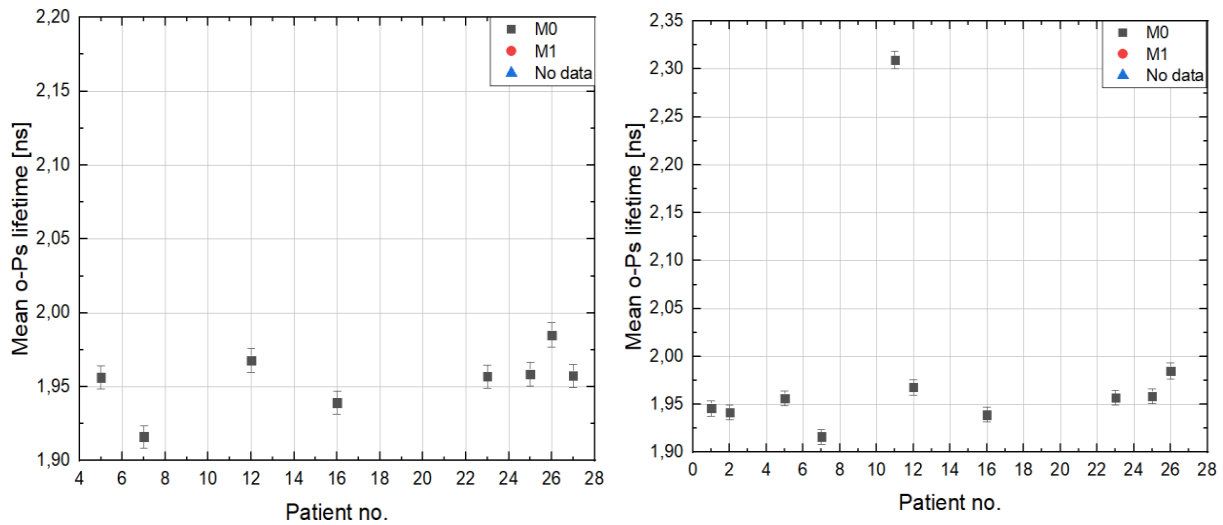


Fig.42. o-Ps dependency of different M characteristic, after including histopathologic results. On the left graph for good results and on the left the average one's were added.

The results for the TNM classification do not show any dependence on mean o-Ps lifetime in cancer tissues, however, after taking into account the histopathological classification, the number of examined patients dropped sharply and therefore no further conclusions can be made.

The last but different type of checked staging system is G classification. Three to four-stage scales of malignancy, depending on the degree of cell differentiation. It is the only one of them that take into consideration difference in structure, and this fact is crucial for PALS method. The results are presented on graph 43 and 44. In measured samples only three kinds of differentiation are observed.

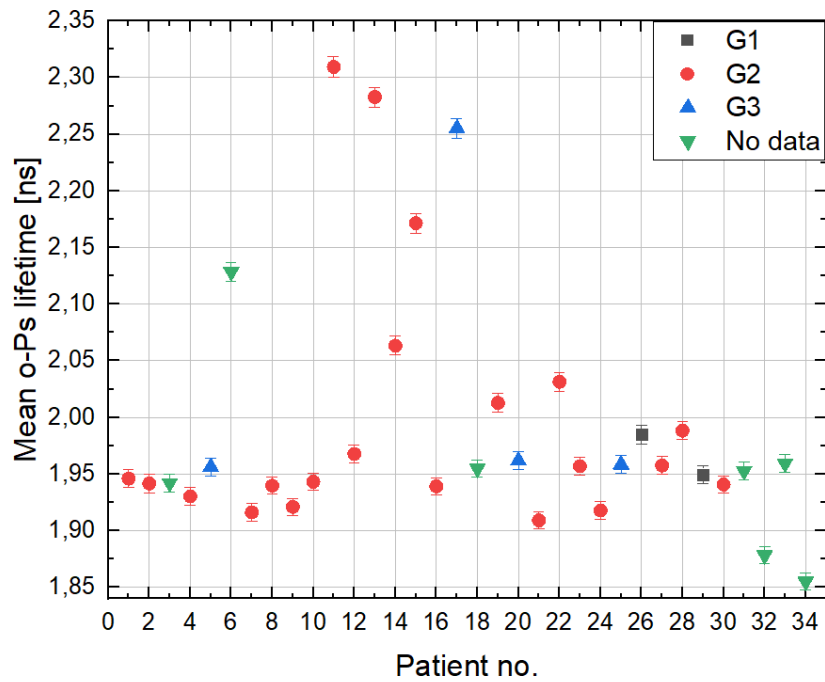


Fig.43. o-Ps dependency of different G characteristic for all patients

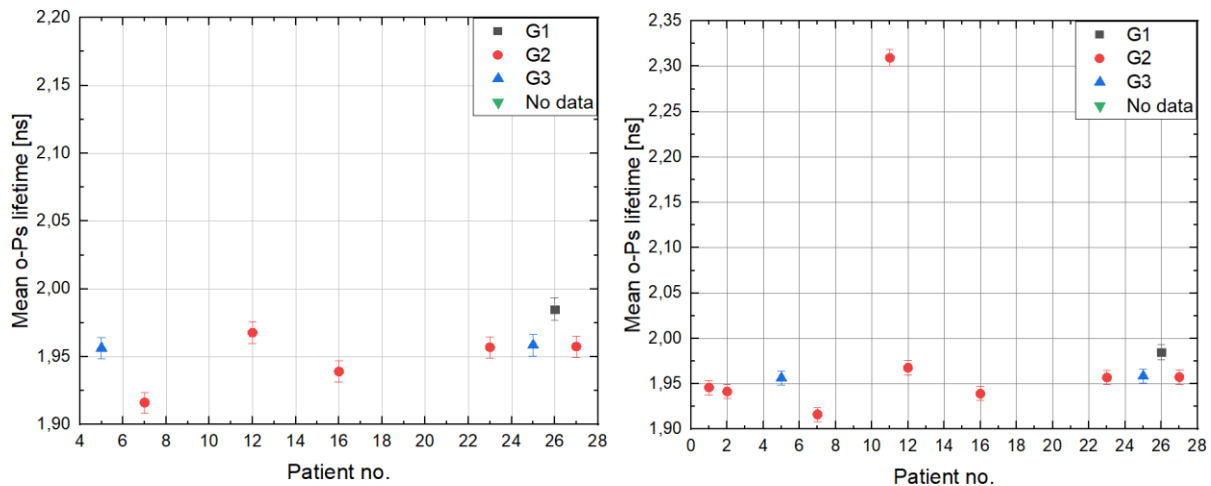


Fig.44. o-Ps dependency of different G characteristic, after including histopathologic results. On the left graph for good results and on the left the average one's were added.

As one's can see, G3 is distinguished by almost identical o-Ps lifetime in cancer tissues, G2 as a differentiated form (some abnormal cells appear in it) shows the greatest divergence. And the G1 which is mostly alike normal cells has bigger lifetime than less differentiated cancers.

5.4. Comparison of results from the J-PET detector and PALS setup.

Studies on fixed normal and cancer large intestine tissue were conducted also on the J-PET detector and then compared to the results obtained from the PALS measurements. Among these 17 of them are men and 10 women. Results for 27 patients are presented in Fig. 45.

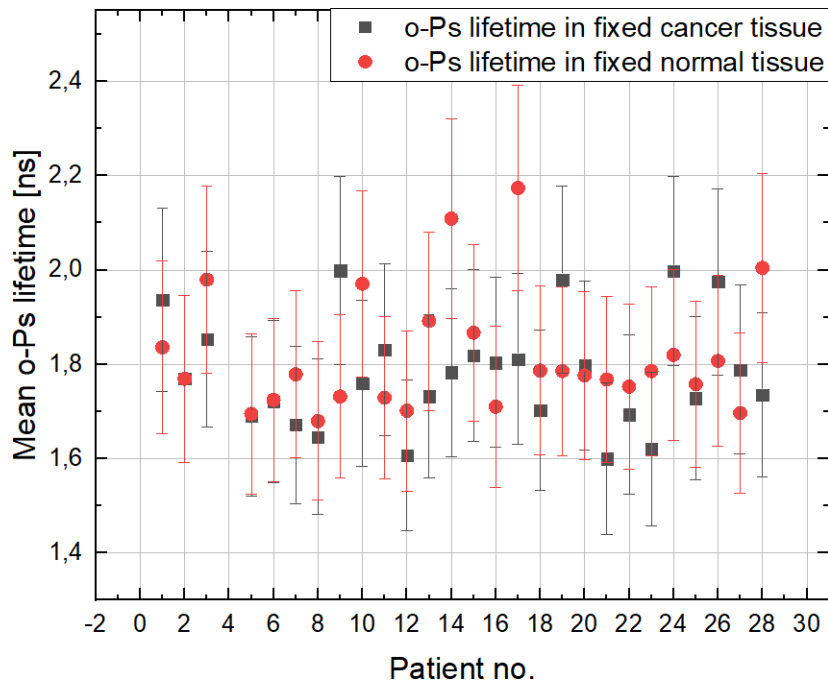


Fig.45. Mean o-Ps lifetime for fixed cancer and normal large intestine tissue measured by the J-PET detector

For 21 out of 27 samples, mean o-Ps lifetime was higher for cancer tissues. Comparison of results obtained by both setups described earlier is shown in Fig. 46.

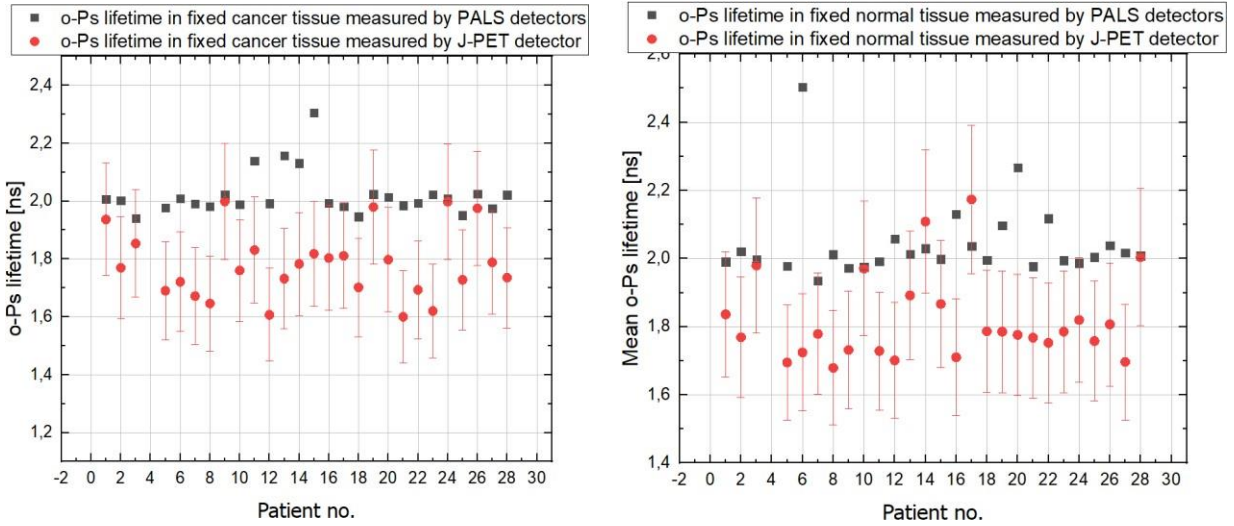


Fig.46. Comparison of results between the J-PET Detector and PALS setup for (left) cancer and (right) normal tissues.

Fig. 45 shows that the mean o-Ps lifetime values obtained for the J-PET detector, are lower than for the PALS setup. This observation can be made for both types of samples (cancer, normal). The results obtained on J-PET scanner are characterized by higher uncertainty [49].

6. Summary and conclusions

Goal of this work was to examine the correlation between orth-positronium (o-Ps) mean lifetime and the degree of malignancy, size, type of cells, and other factors which can be associated with colorectal cancer, contemporaneously demonstrate the potential of simultaneous PALS and PET scan. All of the mentioned factors were examined, and the results were described in this chapter.

Measuring conditions (temperature and humidity) do not affect timing capabilities of the BaF₂ detector. The temperature change from 21.0°C to 24,5°C and the difference between maximum to minimum sigma value is 0,004 ns what is the 3% of the mean sigma value.

From 28 samples only eight of them were marked as samples that consisted mostly expected cells and additionally three patients as samples contained other types of cells. For patients in the same group there is no correlation between its specification and mean o-Ps lifetime.

The TNM classification also did not have any impact, as it studies only the size of the primary tumor or metastasis. As goes for G classification there are some differences. Patients marked as G3 (low-differentiated cancer) had the same mean o-Ps lifetime and G2 (moderately differentiated cancer - cancer cells similar to normal cells) had the largest spread of mean o-Ps lifetime results. G (Grading) determines the shape of the cell, thus can affect the results of structural measurements such as PALS. However, this measurement is based on low number of patients, therefore no further conclusions can be made.

Average of mean o-Ps lifetime for not fixed cancer specimens was equal to 2.01(01) ns, when for not fixed normal tissues it was equal to 2.01(01) ns. For fixed cancer and normal samples, averages were equal to 2.02(01) and 2.04(01) respectively. These results are similar but fixed samples had bigger tendency to that the results converge to a value of 1.8 ns, which is the value of o-Ps lifetime in 4% formalin. Which means that samples after fixation shows similarity to formalin.

Comparison of the mean o-Ps lifetime between the J-PET Detector and PALS system, shown in Fig 45. shows within the errors, results overlap. Low measurements statistic causes higher errors for J-PET detector. Statistic for PALS detectors is around 80 thousand counts while for J-PET scanner the number of counts is around 20 thousand. Statistics for current measurements (on J-PET detector) were collected for 8 hours. Tab. 1 shows the time resolution of PALS setup and J-PET

detector. In order to improve uncertainty of the o-Ps mean lifetime determination, both efficiency and time resolution of the J-PET detector have to be improved.

Table.1. Comparison of the time resolution, obtained from the fitting PAL spectra for 3 examples of fitted samples, expressed as Full Width at Half Maximum of the resolution function.

FWHM [ns]	
PALS	J-PET
0.2984(01)	0.638(12)
0.3010(01)	0.616(12)
0.2972(01)	0.675(15)

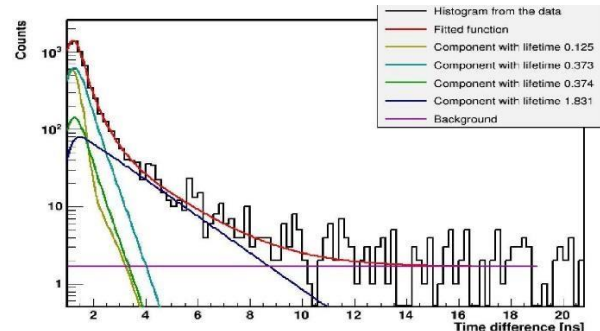
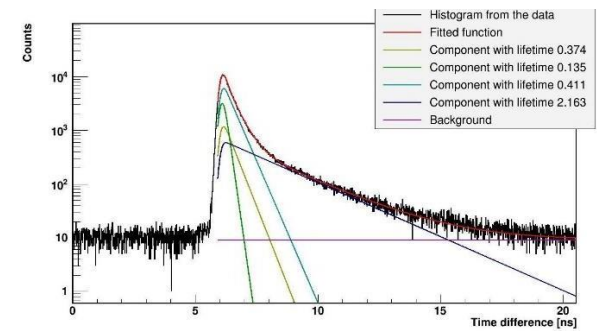
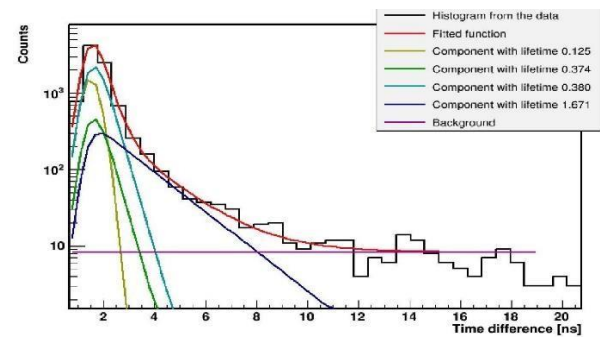
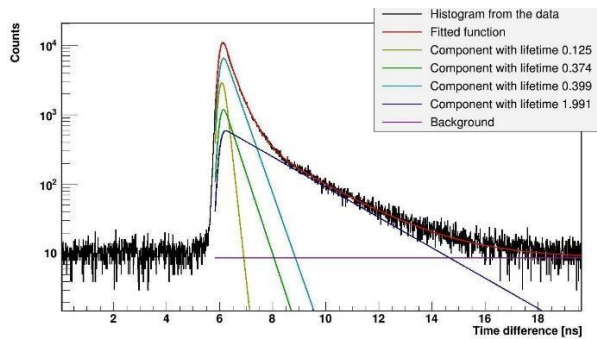
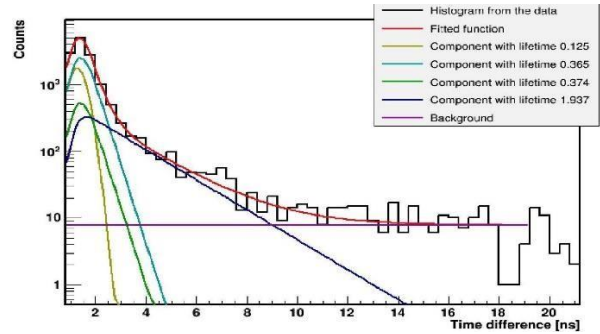
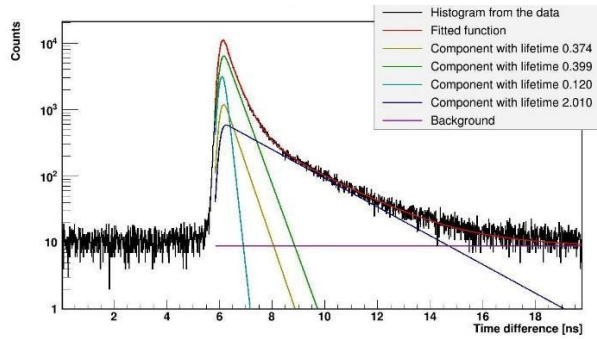
7. Bibliography

- [1] B. Stewart et al., World Health Organisation, ISBN: 978-92-832-0429-9 (2014)
- [2] Moskal, P., Kisielewska, et al., EJNMMI Phys 7, 44 (2020). <https://doi.org/10.1186/s40658-020-00307-w>
- [3] M. Balińska et al., Kosmos 44, Biologia nowotworów; No. 2 (227). ISSN:0023-4249 (1995)
- [4] <https://www.ck12.org/biology/gene-regulation-and-cancer/lesson/Gene-Regulation-and-Cancer-Advanced-BIO-ADV/> Dostęp: 29.06.2020r.
- [5] G.M. Cooper et al., The Cell: A Molecular Approach. 2nd edition. Sunderland (MA): Sinauer Associates; (2000)
- [6] Wiley Blackwell et al., UICC, ISBN: 978-1-119-26357-9 (2007)
- [7] O'Sullivan B et al., Lancet Oncol.18(7):849–851 (2017)
- [8] J. Brierley, CMAJ 174(2):155–156 (2006)
- [9] Hideki Ueno et al., Journal of Clinical Oncology 30:13, 1519-1526 (2012)
- [10] Cancer Research UK <https://www.cancerresearchuk.org/about-cancer/melanoma/stages-types/tnm-staging>
- [11] G. Hounnou et al., Surg Radiol Anat., 24 (5), 290–4. doi:10.1007/s00276-002-0057-y (2002).
- [12] https://commons.wikimedia.org/wiki/File:Layers_of_the_GI_Tract_english.svg?uselang=pl
Dostęp: 10.06.2020
- [13] R. Fodde et al., Nat. Rev. Cancer 1,55-67 (2001)
- [14] H. Gray, Anatomy of the Human Body, Elsevier 40 edition (2008)
- [15] Z. Bura et al., Acta Phys. Pol. B 51, 377 (2020)
- [16] T. Levin et al., Ann. Intern. Med., 145(12):880-6 (2006)
- [17] M. Michel. Ter-Pogossian et al., Radiology. 114 (1): 89–98. Doi: 10.1148 / 114.1. 89.(1975)
- [18] E. Czaicka, praca magisterska: Liniowy model pozytonowego tomografu emisyjnego, UJ 2008
- [19] P. Moskal, ANNALES UMCS Physica 66, 71-88 (2012)
- [20] D.B. Cassidy, A.P. Mills Jr., Nature, 449 (7159), 195-197 (2007)
- [21] E. Kubicz et al., Nukleonika 60(4), 749 (2015)
- [22] Kozłowska, praca magisterska, Copernicus University in Toruń (UMK) 2011
- [23] A.Z. Hryniewicz, E. Rokita: Fizyczne metody diagnostyki medycznej i terapii, PWN 2000.
- [24] <https://commons.wikimedia.org/wiki/File:PhotoMultiplierTubeAndScintillator.svg> Dostęp 30.03.2020r.

- [25] P. Moskal et al., *Inżynier i Fyzyk Medyczny* 4(4), 195-198 (2015)
- [26] P. Moskal et al., US Patent 9851456 (2017), PL 227658 (2013)
- [27] P. Moskal et al., *Phys. Med. Biol.*, 055017, 64 (2019)
- [28] P. Moskal et al., *Phys. Med. Biol.*, 2025, 61 (2016)
- [29] P. Moskal et al., *Nucl. Med. Rev.*, 15, 81-84 (2012)
- [30] S. Niedźwiedzki et al., *Acta Phys. Polon. B* 48, 10, 1567 (2017)
- [31] P. Moskal et al., *Nucl. Instrum. & Meth. A* 775, 54 (2015)
- [32] M. Pałka et al., JINST 12 P08001 (2017)
- [33] G. Korcyl et al., *IEEE Transactions on Medical Imaging*, 37 (11), 2526 (2018)
- [34] M. Skurzok, M. Silarski, K. Kacprzak: J-PET Data Analysis with Framework software version 6.1
- [35] T. Bednarski, Praca doktorska, Jagiellonian University (UJ) (2016)
- [36] S.J. Tao, *J. Chem., Phys.*, 5499, 56 (1972)
- [37] T. Goworek et al., *Chem. Phys. Lett.*, 272, 91 (1997)
- [38] T. Goworek et al., *Chem. Phys.*, 230, 305 (1998)
- [39] M. Eldrup et al., *Chem. Phys.*, 63, 51 (1981).
- [40] P. Moskal et al., *Nat. Rev. Phys.* 1, 527 529 (2019)
- [41] B. Jasinska et al., *Acta Phys. Polon B* 48, 1737 (2017)
- [42] B. Jasinska et al., *Acta Phys. Polon. A* 132, 5 (2017)
- [43] Wadhwa P, Thielemans K, et al. *Methods*. S1046-2023(19)30193-8. doi: 10.1016/j.ymeth.2020.01.005 (2020) [In press]
- [44] D. Kamińska et al., *Eur. Phys. J. C* 76, 445 (2016)
- [45] PET UJ Raport nr 1/2020. Protocol for human tissue PALS measurements.
- [46] K. Dulski et al., *Hyperfine Interact*, 239,40 (2018)
- [47] K. Dulski et al., *Acta Phys. Polon. A* 132, 5, 1637 (2017)
- [48] Pictures made by Ewelina Kubicz and Monika Szczepanek
- [49] K. Dulski, *Acta Phys. Polon. A*. 137. 167-170 (2020)

Appendix A

Examples of spectra for cancer tissues (left) made by PALS detector and (right) by J-PET scanner. The spectra obtained on PALS detectors are characterized by higher statistics than those collected on J-PET scanner. This enables a more accurate parameter adjustment. Information about the fitted parameters are described in Fig.22.



Appendix B

Examples of spectra for normal tissues (left) made by PALS detector and (right) by J-PET scanner. The spectra obtained on PALS detectors are characterized by higher statistics than those collected on J-PET scanner. This enables a more accurate parameter adjustment. Information about the fitted parameters are described in Fig.22.

